Characterization of the Specific Inherent Optical Properties of the Poyang Lake and Quantification of Water Turbidity Using Remote Sensing and a Semi-Analytical Bio-Optical Inversion Model for Shallow Waters

by

Zhou Xichang

Thesis submitted to the International Institute for Geo-information Science and Earth Observation in partial fulfillment of the requirements for the degree of Master of Science in Geo-information Science and Earth Observation, Specialisation: Geo-information for Natural Resource and Environment Management

Thesis Assessment Board

Prof. Dr. Ir. Alfred de Gier, Chairman (ITC)
Prof., External Examiner (Tsinghua University)
Dr. Michael Weir, Course Director (ITC)
Prof. Dr. Du Qingyun (SRES)

Supervisors: Dr. Suhyb Salama (ITC), Prof. Du Qingyun (SRES)

INTERNATIONAL INSTITUTE FOR GEO-INFORMATION SCIENCE AND EARTH OBSERVATION

ENSCHEDE, THE NETHERLANDS

SCHOOL OF RESOURCES AND ENVIRONMENTAL SCIENCE (SRES)

WUHAN UNIVERSITY, CHINA

Disclaimer

This document describes work undertaken as part of a programme of study at the International Institute for Geo-information Science and Earth Observation. All views and opinions expressed therein remain the sole responsibility of the author, and do not necessarily represent those of the institute.

Abstract

Poyang Lake has great ecological value for birds' conservation. However, the hydrology condition has been badly affected by dredging. Thus, monitoring water turbidity is of consequence. This study aims to characterize the specific inherent optical properties (SIOP) of the Poyang Lake and quantify water turbidity using Semi-Analytical Bio-Optical model both with and without bottom reflectance for shallow waters.

The GSM (for Garver-Siegel-Maritorena) model has been applied to retrieve the inherent optical properties (IOP) from the measured remote sensing reflectance and the SIOP can be calculated using the in situ concentration of Chlorophyll-a (Chl-a) and suspended particles (SPM). Considering the model used non-linear regression, the uncertainties of the retrievals were derived. The bottom reflectance was then added into the model to research the impact of bottom reflectance. After the preprocessing of MERIS (Medium-spectral resolution imaging spectrometer) images, the algorithm from the inversion of models was applied to images to achieve the map showing the SPM concentration of Poyang Lake.

A strong linear relationship (R^2=0.85) between the retrieved IOP and the measured SPM concentration was built. For Chl-a, the relation (R^2=0.68) was not as good as for SPM. This calculated SIOP was then validated with the other half of water samples. The retrieved IOP, together with this SIOP, gave the result of concentration of SPM and Chl-a. The calculated concentration of water constituent fit the measured SPM very well. Adding bottom reflectance did not improve the establishment of SIOP with weak relation for water components. In validation for SPM, it is not obvious that which model, with or without bottom reflectance, contained less error. The GSM model and the linearly retrieved SIOP were applied to the image to obtain the map showing the SPM concentration. The map retrieved by this method is invalid since there are much less pixels remaining in the lake area. The neural network method in BEAM is thus used to retrieve the map. The map indicated a high concentration area around the dredging activities frequently happening place.

Many factors may contribute to the unsuitable way of adding reflectance which included the acquirement of bottom spectrum and the measurement of bottom depth, etc. The basic reason is the limitation in bands selected into the model. Thus this needs further research. Additionally, time series images were needed to assess the change of water turbidity.

Acknowledgements

At the end of my study period in ITC and the finishing of this thesis, I would like to express my hearty thanks to the institutes and persons who have given me generous support during this time.

I am especially grateful to the Department of Natural Recourse Management in ITC who provide me a chance to study there. The experience in the Netherlands had broadened my view and expanded my mind. The teachers and classmates there are also appreciated for their friendship which brought me a warm environment in those homesick days.

My deepest thank goes to Dr. Suhyb Salama, my ITC supervisor, not only for his timely guidance and valuable supervision, but also for his support and encouragement whenever I encountered problems. Another reason why I feel so fortunate to carry out my thesis under the supervision of him is his specialist in the techniques and the critically attitude in the scientific research. Grateful thanks to my Wuhan supervisor, Prof. Du Qingyun for his support and suggestions which offers me advices to improve the research. Additionally, his help on the accessing of requirements for field work is significant.

Special thanks are addressed to Dr. Wu Guofeng for his generous help on almost each step of my research. Prof. Chen Xiaoling is also the teacher I would like to thank for her widely knowledge on Poyang Lake. I would like to appreciate the suggestions provided by people in the Protection Station of Poyang Lake which give me useful information on field work.

My genuine thanks go to Prof. David Rossiter who is always there to help and trying his best to teach us improving English both in the time we were in the Netherlands and when we are back in China. Thanks to my Chinese colleagues who were together with me in the Netherlands. Those cherish memory will be always in my mind.

Finally, I would like to thank my family. Your confidence in me makes me confidence in myself to solve all the problems and your support and encouragement make me have the courage to face a bright future!

Table of contents

List of figures

List of tables

List of frequently used abbreviations

SABO	Semi-analytical bio-optical
SPM	Suspended Particles Materials
CDOM	Coloured Dissolved Organic Material
Chl-a	Chlorophyll-a
IOP	Inherent Optical Properties
SIOP	Specific Inherent Optical Properties
AOP	Apparent Optical Properties
R_{rs}	Remote sensing reflectance
b_{bp}	baskscattering coefficient of SPM
a_{ph}	absorption coefficient of Chl-a
a_{dg}	absorption coefficient of CDOM
CI	Confidence intervals
R^2	R Square
RMSE	Root Mean Square Error
SRES	School of Resource and Environmental Science
WEPI	Wuhan Environmental Protection Institutes
MERIS	Medium-spectral resolution imaging spectrometer
MODIS	Moderate-resolution Imaging Spectroradiometer
SSC	Suspended sediment concentration
PL	Poyang Lake

1. Introduction

1.1. Background

Poyang Lake is the largest fresh lake in China and it has great ecological value (Center for Remote Sensing/GIS Application of Jiangxi Province 2003). Being a natural wetland with mild climate and intensive rainfall, Poyang Lake is one of the biggest birds' conservation areas in the world (Wu et al. 2007). The lake is an important habitat for some endangered migratory birds especially during the winter (Li et al. 2005). These birds feed on the tubers of submerged aquatic vegetation (Senar and Borras 2004); therefore, conservation of the vegetation growth and wetland environment is of consequence.

Recently, hydrological conditions of Poyang Lake have been badly affected by many factors (Wu et al. 2007). Sand dredging is one of these factors that Poyang Lake has suffered from (Wu et al. 2007). Reports (Zhong and Chen 2005; Fok and Pang 2006) have indicated that sand dredging reduces the water clarity in the northern part of the Poyang Lake and thus has a negative impact on this ecosystem since 2001.

Monitoring and control of the water turbidity is important for the protection of the Poyang Lake ecosystem. When water turbidity increases, the available light for the submerged aquatic vegetation will decrease (Wu et al. 2007). Since there is not enough light for the growth of such vegetation, the migratory birds feed on the tubers of this kind of vegetation may lack of food source. Although there are many causes of the decreasing of light for the under water vegetation such as algae, water turbidity caused by dredging is significant since 2001. As a result, it is crucial to monitor the water turbidity to provide information for further management.

Remote sensing offers possibilities to monitor the distribution of sediment concentration in water. There is a relation between water leaving radiance and water composition (Kirk 1994). Using remote sensing methods, water turbidity can be estimated from satellite images. This will facilitate the assessment of the spatial and temporal patterns of suspended sediments (Liu and Rossiter 2008).

1.2. Research Problems

The Inherent Optical Properties (IOP) are the properties that only depend on the medium thus are independent of the light field within the medium while the Apparent Optical Properties (AOP) are the properties that both depend on IOP and the ambient light field. The AOP that are used frequently are Irradiance Reflectance, Remote Sensing Reflectance and Diffuse Attenuation Reflectance.

The IOP are comprised by three parts: Absorption, Scattering and Remittance. Table below shows the processes that contribute to these IOP. The IOP, the spectral absorption and scattering coefficients, can be also identified as spectral absorptance and scatterance in the medium per distance. The sum of absorption and scattering is the spectral beam attenuation. In the equation 1-1 and 1-2, a and b are the absorption and scattering coefficients while A and B are the absorptance and scatterance respectively. λ means wavelength and γ is distance.

$$a(\lambda) \equiv \lim_{\Delta r \to o} \frac{A(\lambda)}{\Delta r} \quad (m^{-1}), \tag{1-1}$$

$$b(\lambda) \equiv \lim_{\Delta r \to o} \frac{B(\lambda)}{\Delta r} \quad (m^{-1}), \tag{1-2}$$

Table 1-1Processes that affect reflectance

Absorption	Scattering	Remittance
Water molecules	Water molecules	Raman scattering
Phytoplankton	Organic particles	Fluorescence by phytoplankton
Dissolved organic matter	Mineral particle	Fluorescence by yellow matter
Organic detritus	Air bubbles	Bio-luminance
Particles		

For case 2 water, the main water components are phytoplankton, CDOM and suspended particles(IOCCG 2000). Like most of inland waters, Poyang Lake is case 2 water i.e., water that contains mainly two constituents. One of these constituents is dissolved organic matter which means colored dissolved matter (CDOM) and the other one is suspended particles both in biological and physical. In this work we neglect the absorption of suspended particles other than the green pigment, i.e. chlorophyll-a. In other words, the absorption of suspended matter arises from the chl-a in phytoplankton. This is of course a crud approximation. However the absorption of non algae particles is similar in shape to that of CDOM and difficult to be deconvolved form it. Therefore in this research, the absorption coefficient ($a(\lambda)$) is due to water absorption ($a_w(\lambda)$), phytoplankton absorption ($a_{ph}(\lambda)$) and ($a_{dg}(\lambda)$) which is the combination of colored detrital and dissolved material (CDM) (Carder et al. 1991; Nelson et al. 1998; Nelson and Siegel 2002). The scattering coefficient ($b(\lambda)$) is the sum of water scattering ($b_w(\lambda)$) and the suspended particles scattering ($b_{bp}(\lambda)$).

The Specific Inherent Optical Properties (SIOP) is the amount of absorption/scattering per unit concentration. It can be simplified identified as: SIOP=IOP/concentration (Bukata et al. 1995). Having this SIOP, together with models, researchers can derive either IOP or concentration.

The considered Semi-analytical bio-optical (SABO) model in this study is the GSM model developed by

Garver-Siegel-Maritorena (Maritorena and Siegel 2006). We will refer to as the GSM model throughout the manuscript.

Up to now the specific inherent optical properties (IOP) of the Poyang Lake have not directly or indirectly been measured. Knowledge about the values of SIOP is essential to derive reliable estimates of SPM concentration.

Many studies have already been applied to monitor sediment concentration in Poyang Lake but all of them used empirical or statistical models (i.e. neural network) and so far little research has been done in applying semi-analytical bio –optical (SABO) model to this specific area. In the empirical or semi-empirical way, only the above water reflectance and the sediment concentration are linearly or nonlinearly linked and are taken into consideration which therefore leads to low accuracy since many other factors in water such as phytoplankton and colored dissolved material (CDOM) have been ignored.

So far no attempt has been made to add the bottom reflectance in the models in Poyang Lake. Poyang Lake becomes shallow during the dry season (Wu et al. 2007). As a result, the bottom reflectance will affect the observed reflectance. Because the water level of Poyang Lake differs a lot in wet and dry seasons, the bottom reflectance has a large effect on above water reflectance in these seasons. Consequently, no previous researches have considered bottom type of this lake which may cause the inappropriate way of using such model in different seasons.

Therefore in this study, we will search for the methods to solve the above mentioned problems. Firstly, we will apply the SABO model using the measured reflectance in the field work to derive the inherent optical properties (IOP). Case 2 water will be considered in this study (Morel and Gordon 1983). The considered IOPs for the PL are: (1) absorption coefficient of the water molecules; (2) phytoplankton absorption; (3) CDOM absorption; (4) the backscattering coefficient due to water and suspended materials (SPM) (Morel and Gordon 1983). Secondly, the model will include the effect of bottom reflectance. We will apply the model with the effect of bottom reflectance to retrieve IOP again using the field data. Also, uncertainties analysis of the retrieved IOP will be carried out. The purpose of deriving uncertainties is to check the performance of the SABO model for the Poyang Lake. Additionally, the SIOP can be derived from estimated IOP and measured concentrations of the water components with and without the effects of bottom reflectance. Based on this comparison, the pros and contras of adding bottom reflectance will be explored. Then, maps detailing the spatial distribution of suspended sediment will be produced for the Poyang Lake. These technique and maps will help on assessing the impact of ceased dredging activities, since the year 2008, on the Poyang Lake water clarity.

1.3. Research Objectives

1.3.1. General Objective

The main objective of this research is to characterize the specific inherent optical properties of the Poyang Lake and quantify water turbidity using remote sensing and Semi-Analytical Bio-Optical model for shallow waters.

1.3.2. Specific Objectives

- To calibrate and validate a Semi-Analytical Bio-Optical Model (SABO) for Poyang Lake.
- To obtain the uncertainties on the derived products.
- To add shallow water component that considers bottom reflectance to the model.
- Build up a library of the specific inherent optical properties (SIOP) of the Poyang Lake.
- To assess the spatial water turbidity variation by applying the above steps on MERIS images.

1.4. Research Questions

The research questions in this research are:

- Is it feasible to calibrate the semi-analytical ocean color model for inland waters?
- What are the uncertainties in this semi-analytical model for inland lake?
- Can we build up SIOP of Poyang Lake that is valid for other researches?
- What is the effect of bottom reflectance on optically clear waters? Do we need to add the bottom effects?
- What is the spatial variation of water turbidity in Poyang Lake?

1.5. Assumptions

This research is based on the assumptions below:

- The SIOP of Poyang Lake is linearly related to IOP.
- The SIOP of Poyang Lake is constant.
- There is one bottom type in Poyang Lake.
- The spectral shape of bottom reflectance is derived from images.

1.6. Research Approach

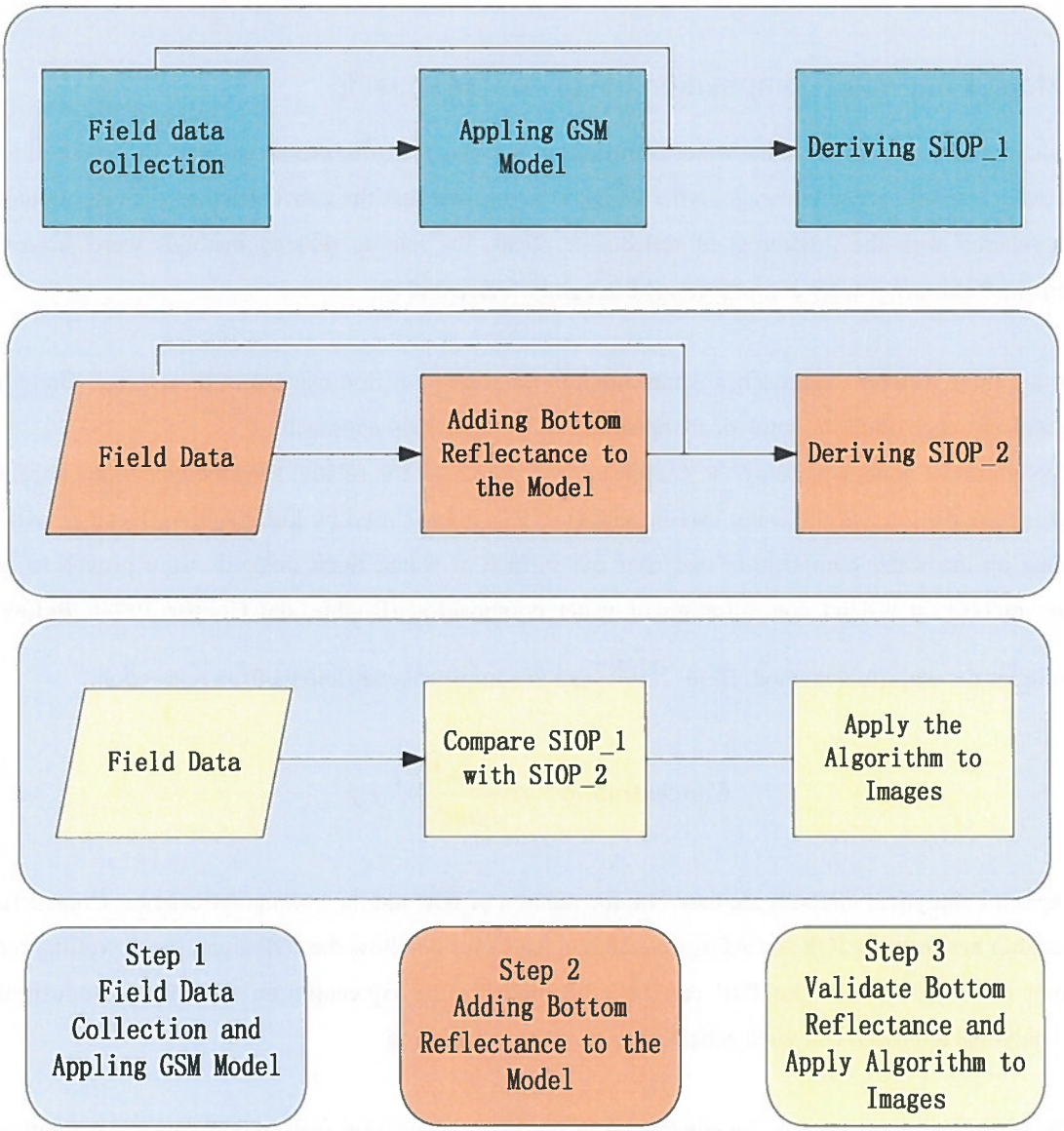

Figure 1-1 Structure of the study

2. Literature Review

2.1. Monitoring water composition using remote sensing

The traditional way to monitor the water composition is through in-situ measurements. This method is costly and covers a small spatial coverage. Afterwards, it was found that the concentrations of water composition had a relation with the brightness of reflectance. Thus, the remote sensing methods were proved to be feasible in monitoring water composition (Miller and McKee 2004).

There are three different approaches when monitor water composition using remote sensing. These are the empirical approach, the semi-analytical approach and the analytical approach.
(1) The empirical approach, being the simplest one, is based on the relationships between the concentration of water composition and the water leaving radiance. It is always used by linking the reflectance with the in situ data on the water composition that near the surface of water. Such methods were proved to provide enough precise on predict concentration of water composition (Ritchie and Cooper 1998). Below is an example for the empirical method. Here α, β, γ are the empirical coefficients from regression.

$$Concentration = \alpha(\frac{band1}{band2})^{\beta} + \gamma \quad (2\text{-}1)$$

(2) The semi-analytical methods are based on the relation of IOP and the volume reflectance. Considering the relationship between the IOP and AOP, this method has described how the IOP affect the upwelling radiance (Gordon et al. 1975). As the IOP can be computed by the concentration of water composition, the semi-analytical approach can yield satisfactory result on monitoring.

(3) The analytical approach can be considered as an analytic function that could express the relation. The volume reflectance is a function of IOP of water constituents and the model is a solution to this equation.

The analytical approach has high demands on the in situ measurements because the filed data instead of empirical values are applied to adjust the model. It can bring the advantage that for a specific region; the model can fit best and give accuracy result. However, this approach also has big limitation of the requirement on the in situ data to build the model which will always cost a lot so that it is sometimes not very feasible.

2.2. Semi-analytical method for shallow inland water

It has been proved that there is a relation between remotely sensed radiances and water composition (Kirk 1994). From Kirk's work we can learn that the photons are either absorbed or scattered by water. The absorption and scattering properties only depend on the substances that comprise the water medium thus they are named inherent optical properties (IOP). The remote sensing reflectance can be linked to IOP as $R \equiv f^0 \frac{b_b}{a+b_b}$.

For deep water, there is a simple relation of

$$\text{Reflectance} \propto g \frac{backscattering}{backscattering + absorption}$$

which expresses proportion to the backscattering and inversely proportion to the absorption. But for shallow water the effect of bottom should also be taken into consideration. Since the main significance of upward radiance is based on the optical properties, the remotely sensed radiances can tell about the concentrations of the optically significant constituents in water (Kirk 1994).

The relation between IOP and reflectance spectra in turbid inland lake has be measured and tested in later researches. A linear backscatter albedo model which illustrated the relation between subsurface irradiance reflectance, absorption and backscattering was investigated as $R(0-)=r1b_b/(a+b_b)$. And in previous researches, the r1 has been estimated to be from 0.12 to 0.56 for the water types of shallow eutrophic lakes, shallow mestrophic lakes and deep lakes (Dekker et al. 1997). Thus the TOA reflectance can be used in radiative-IOP transfer models to simulate ranges of concentrations. The models then can be used to yield maps from AOP to the related water composition concentration.

2.3. Bio-Optical model for inalnd water

The major factors that affected water quality contained SPM, Chl-a and CDOM (Ritchie and Schiebe 1998). Bio-Optical models described the contributions of these factors to the light attenuation(Bukata et al. 1995). Thus the models can help to build the relation between the remote determinations of water color and the water composition.

For SPM, there are many factors that contribute to the surface water radiance which included sediment texture, colour and type (Ritchie and Schiebe 1998). This surface water radiance increased in the visible and the near-infrared band(Ritchie et al. 1996). The impact of SPM on volume reflectance was obvious (Bukata et al. 1995). IOCCG (2006) indicated that the absorption of Chl-a had two absorption peak at the wavelength around 440nm and 665nm. Kirk (1994) mentioned that CDOM absorbed light in both ultraviolet and visible

bands. The strong absorption occurred in the blue (IOCCG 2006).

Gordon and Morel (1983) had characterize particle scattering as $b_{bp}(\lambda)=0.30(550/\lambda)C^{0.62}$ while C was the concentration of SPM. For Chl-a, the concentration can up to 100mg/m^3, the relation was defined as $aph(\lambda)=aph^*(\lambda)C$ while C was the concentration (Bricuad et al. 1995). For CDOM, $adg(\lambda)=adg(\lambda_0)EXP(-S(\lambda-\lambda_0)$ with the range of S from 0.011 to 0.021nm^{-1}(Carder et al. 1991).

2.4. Monitoring SPM concentration in Poyang Lake

Studies on the sediment concentration of Poyang Lake mostly focused on using empirical models combined with Remote Sensing images to derive distribution map. Wu et al. (2007) has developed a regression model describing the relation between Secchi disk depth and red bands of Landsat TM images (Wu et al. 2007). Liu and Rossiter (2008) have built a regression model between concentration of suspended sediment and bands in MODIS and have proved that the first band in MODIS is best in regression (Liu and Rossiter 2008). They also shows that there are more suspended sediment in the northern part of the lake and compares the variation of sediment concentration in the condition of different of water level and multi-temporal water patterns. Chen et al. (2007) has used a semi-empirical model to argue that after comparison of different bands or ratio of bands, they found the seventh band in MERIS is most appropriate for the logarithm regression of suspended sediment(Chen et al. 2007).

2.5. Characteristics of MERIS

MERIS (Medium-spectral resolution imaging spectrometer) is a sensor on board of Envisat. It has 15 bands from visible to infrared centered at 412nm to 900nm. From the official website of ESA(European Space Agency 2000-2009), we can obtain the information that MERIS instrument can acquire data at illumination conditions over the world. It scans the Earth, with using a "push-broom" scanner covering a swath width of 1150km using its 68.5° field of view.

The MERIS product contains three processing levels which are level 1B, level 2 and level 3. The L1B level provides calibrated spectral radiance at TOA so that it has 15 different bands. The L2 level is geophysical parameters derived form L1B. L3 level is a synthesis of many MERIS products which can be considers as the spatial and temporal integration of level 2. Meanwhile, it produces map projection (European Space Agency 2000-2009).

There are also three different types of resolutions in MERIS images. The pixel size in Full Resolution (FR) is 260m×290m; in Reduced Resolution it is 1040m×1060m which is the integration of FR data; this pixel size

goes to 4160m×4640m in Low Resolution images. Accordingly, the FR image has 4×4 more points than RR while RR has 4×4 more points than LR in the same image.

Table 2-1Basic characters for MERIS bands

Band	Wavelength(um)	Bandwidth(nm)	Revisit time(days)
Band 1 (VIS)	0.4125	10	3
Band 2 (VIS)	0.4425	10	3
Band 3 (VIS)	0.49	10	3
Band 4 (VIS)	0.51	10	3
Band 5 (VIS)	0.56	10	3
Band 6 (VIS)	0.62	10	3
Band 7 (VIS)	0.665	10	3
Band 8 (VIS)	0.68125	7.5	3
Band 9 (VIS)	0.705	10	3
Band 10 (VIS)	0.75375	7.5	3
Band 11 (VIS)	0.76	2.5	3
Band 12 (VIS)	0.775	15	3
Band 13 (NIR)	0.865	20	3
Band 14 (NIR)	0.89	10	3
Band 15 (NIR)	0.9	10	3

(Source: http://www.itc.nl/research/products/sensordb/getsen.aspx?name=MERIS)

The applications of MERIS occur at Oceans, Atmospheric and Land. The MERIS instrument is firstly and mainly designed to observe the colors of oceans and combined with models, it can predict the quality of oceans which can help people to monitor changes. One important advantage of MERIS compared with other satellite images such as Landsat and MODIS is that it can provide information on atmospheric parameters directly to improve the study on cloud sand water vapour. For clouds, the scattering coefficient for the wavelength of 753.75nm is used(Fischer et al. 2000). For water vapour, the method is relating the columnar water vapour content to the ratio of MERIS channels 14 and 15 (Fischer et al. 1997). Additionally, it is widely applied on observing land surface especially vegetations.

Since MERIS is born to detect oceans and it includes atmospheric features in, it is considered that MERIS can be better used than some other satellite images on observing water. Duan and Zhang (2008) has proved that MERIS can predict the cyanobacteria bloom better than MODIS in Finland costal line (Duan and Zhang 2008). Li et al. (2006) argued that the 5th, 12th, 13th band can be effectively used to derive SSC in Taihu Lake in China (Li et al. 2006).

3. Study area and materials

3.1. Study area

3.1.1. Location of Poyang Lake

Poyang Lake is located at latitude 28°22′- 29°45′ north, longitude 115°47′- 116°45′east. It lies in the northern part of Jiangxi Province, at the southern bank of the middle and lower reaches of Yangtze River(Center for Remote Sensing/GIS Application of Jiangxi Province 2003). We can easily find the locations by the maps below. The Jiangxi Province is in the southeast of China and the north part of Poyang Lake is connected with the Yangtze River. The lake is comprised of nine sub lakes which are: Dachahu, Dahuchi, Changhuichi, Xianghu, Zhushihu, Banghu, Shahu, Zhonghuichi and Meixihu.

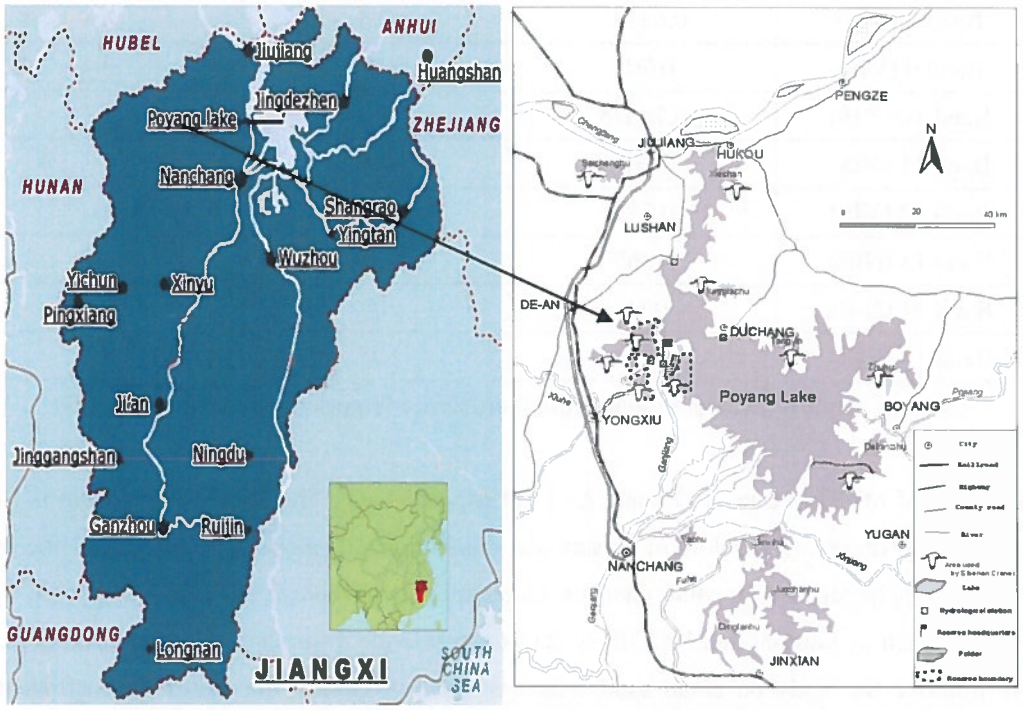

Figure 3-1Maps of China, Jiangxi Province and Poyang Lake
(Source: http://www.scwp.info/china/poyanglake.shtml)

3.1.2. Hydrology conditions

According to the specific location of Poyang Lake, the climate there is a warm, humid, subtropical climate and appropriate for living organisms. The average temperature of the whole year is from 10 to 20 centigrade and differs from 3 to 36 centigrade in winter and summer. There is abundant rainfall in summer but not in winter and annual mean precipitation is from 1400 to 1700mm(Center for Remote Sensing/GIS Application of Jiangxi Province 2003).The table below shows the average water level in the 12 months in the year from 1956 to 2005 at Hukou where the lake is deepest (Liu 2006). It is obviously that the water level fluctuated a

lot with the change of seasons, indicating that in dry season which was from November to April it was low while in wet season which was from May to October it appeared high. Based on these data, we can deduce that since the construction of The Three Gorges at 1997, water level of Poyang Lake has decreased but the change following the season remained. Moreover, the lake area can reach 2500km^2 in wet but fall to 1158km^2 in dry which leads to in winter some bottom expose so that this area becomes wet land.

Table 3-1 Monthly average water level from 1956 to 2005

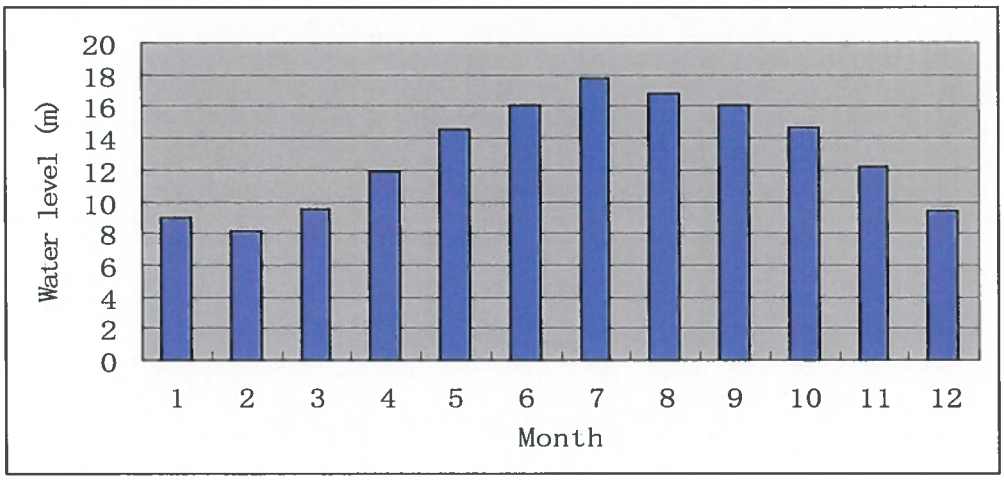

(Source: Liu 2006)

3.2. Research materials

3.2.1. Field data

The in situ measurements are of significance in this research. The field data which were recorded here are water leaving reflectance, the concentration of suspended particles materials (SPM) and concentration of chlorophyll-a (Chl-a). In almost every step we will use the in situ data in the methodology. Basically, they will be applied in two aspects. In the forward process, which means both in the GSM and the adding bottom reflectance process, we will apply the in situ water leaving reflectance into the model to predict IOP and then compute the SIOP with the measured concentration. In the inversion, the in situ data are used to validate the model and compare the results from those two models. The details in field data collection are in the later chapter.

3.2.2. Satellite images

Nine bands in MERIS images, which centered at 410nm, 440nm, 490nm, 510nm, 560nm, 620nm, 660nm, 680nm and 710nm, are used in this research. Both full resolution (300m×300m) and reduced resolution (1.2km×1.2km) are available, indicating that the images contain the top of atmospheric radiances and the core geometric information. Besides, the images also provide data such as meteorological data, terrain height,

the Sun and viewing geometry and the flags that describing the quality and the validity of the images.

Table 3-2 Dates of MERIS images used in this research

Image No.	Level	Resolution	Dates
1	Level 1b	Full	16_Oct_2008
2	Level 1b	Reduced	16_Oct_2008

4. Field data collection

In situ data used in this research contains two parts, one is the remote sensing reflectance measured in the field and the other is the concentration of water components that measured in the lab.

Table 4-1 Data collected and Objectives

Data Collected	Objectives
Remote sensing reflectance	Applying into GSM model and the model of adding bottom reflectance
Concentration of SPM	Deriving SIOP and validate the SIOP
Concentration of Chl-a	Deriving SIOP and validate the SIOP

4.1. Field survey

In this research, 30 samples were chosen according to the result of Liu's (2006) thesis. As the dredging activity mainly occurs at the northern part of the lake, there will be more sampling sites in this area to emphasize the variation of water turbidity. The main principles of locating these samples contains two parts; one is to let the concentration of SPM range from low to high and the other is to make the samples locate as far as possible to ensure them in different pixels in the image. Based on the reasons above, the locations of samples chosen in this study range from 29°15.394′N, 116°04.430′E to 29°15.908′N, 116°03.726′ E. Meanwhile, each two samples have a difference of at least 0.5′ N or E which leads to the interval of them is more than 1km. As in MERIS, the FR images have a resolution of approx 300m×300m, the distance between each two samples is large enough. The figure 4-1 shows the result of Liu's thesis on SPM concentration on November, 2004. Different color presented the difference in the concentration which gave us information on choosing samples that can cover all the range. The white dots in the map show the locations of my sampling points.

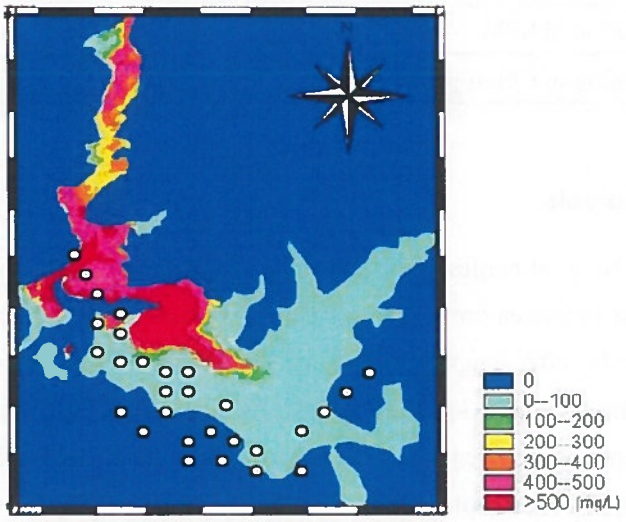

Figure 4-1 Locations of samples

Before the field campaign, the following were prepared: A ASD spectrometer whose electric quantity can last for 3 hours if is continuous used; a laptop with two batteries who can last for 6 hours; 60 plastic bottles with the capability of 600ml each; two big boxes and one of them contains ice; a portable GPS.

The field work was conducted on 15th to 19th October. At each sampling site, firstly, the remote sensing reflectance was measured. The way to measure is based on Tang's research (2004) which contains eight steps. 1) Preheat the spectrometer. 2) Measure the dark current. 3) Measure the standard plate. 4) Measure the standard plate when keeps out the direct sunlight. 5) Measure the target. 6) Measure the skylight. 7) Measure the standard plate. 8) Measure the standard plate when keeps out the direct sunlight(Tang et al. 2004). When we measured the water surface, the sensor of spectrometer is 20cm above water surface and 135°against the sun and 40°against water surface(Mueller et al. 2003). There should be a certain distance between the motorboat and the sensor to avoid the effect from the shallow of boat. At each location, the measurement has been taken for at least 10 times so that we can use the average value. But for each single measurement, it should be finished within 100-200ms to ensure that the sunlight is sustained. Then, using a water sampler, we pumped the water which was 0.5m below the surface into two plastic bottles, citing them and putting them in the different boxes. The box with ice in is for the measurement of Chl-a otherwise the concentration will change in several hours. In the opposite, the concentration of SPM can be stable for several days in room temperature(National Environmental Protection Bureau 2006). Besides, fill the template table of field work with time, location and water temperature.

Table 4-2 Template table of field work

No. of sample:	**Time:**	**Locations:**	**Water temperature:**
To be measured in the field		**Value**	
Above water remote sensing reflectance			
To be measured in the lab			
Concentration of SPM			
Concentration of Chlorophyll-a			

4.2. Laboratory analysis

We have obtained two boxes of bottles from field campaign. One is for the experiment of Chlorophyll-a thus these 30 bottles were in a close environment of 4°C for less than one day. The other is for the experiment of SPM. Each time, at the day after sampling, which meant 16th and 20th Oct, we sent this box of water samples to Wuhan Environmental Protection Institute (WEPI). As they had better devices of centrifugal machine and electronic balance for these experiments than the school of Resources and Environmental Science (SRES) in Wuhan University, they did the whole measurements on concentration of Chl-a and the weighing part of SPM.

The filtering part of SPM was done in the laboratory in SRES. The instruments needed in filtering are: 30 filtration membranes whose pro-size was 0.2um each inside weighing bottles; one filter; one gas regulator; one forceps; one 250ml-graduated cylinder and some distilled water. Among them, the weighing bottles with filtration membranes in have been labeled and the weights of them have been recorded by WEPI before filtering.

(1) The filter and cylinder were cleaned by distilled water every time before filtering otherwise there may remain some sediment which would affect the result. To wash the test glass, 10ml distilled water were used three times for each sample.
(2) Linking the filter with the gas regulator. The upper part of the filter was used to let water samples pass though the membranes which was fixed in the middle of the filter. The lower part of it was a close environment with the gas regular. A piece of filtration membrane was taken outside from the weighing bottle and put on the filter with the labeled side facing down. All the steps that concerned filtration membrane should be done using forceps to avoid directly touch by hand. Then the whole apparatus was fixed. The function of gas regular was that when it was linked with the filter, by reducing the gas in the lower part of the filter, the water samples can pass the membrane otherwise they will remain in the upper part.
(3) Shaking water samples to make the sediment evenly before pouring it into test bottle. Every time the cylinder was used to extract 150ml water sample pass through the membrane first. One important step was reducing the gas in the downward part of the filter. If this water could pass smoothly, it indicated that the water was relatively pure so that more sample water was needed until the water sample can hardly pass the membrane. On the opposite, the sample could hardly passing through the membrane, suggested that this sample was turbid. It was necessary to make sure that the sediment remained on membrane was enough for weighing to avoid much error. In this experiment, the volume of water sample differs from 100ml-400ml.
(4) The gas regulator could be released then in order to take off the membrane from the filter. The forceps was used to fold it and put it into weighing bottle. What should be careful were that the forceps was forbidden to touch the sediment and the filtration membrane could not be broken.

The weighing bottles containing filtration membranes after filtering were sent to WEPI for drying and weighing. Since WEPI got the weighing result of those weighing bottles before and after the filtration, the difference between them indicated the weight of sediment on the membranes. The sediment concentration was thus calculated by the division of weighing difference and the sample volume. The measurements of the concentration of Chl-a were based on "Methods on monitoring water and sewage" authorized by the National Environmental Protection Bureau (NEPB).

5. Methodology

5.1. General description

The preparation part of this research contains three stages which are literature review stage, field campaign stage and satellite images processing stage. The literature review has been continually carried out throughout the entire research. From what we have in that chapter, we will use the remote sensing approach to monitor the water quality and emphasize the utility of semi-analytical methods for shallow inland lakes. After the field campaign and associated laboratory experiments, we have obtained the in situ data of remote sensing reflectance and concentrations of SPM and Chl-a in 30 pairs. The preparation is finished when images which cover the period acquired in this study have been gained.

In chapter one I have showed a brief structure on research approach and the figure 5-1 gives a description on research method in detail.

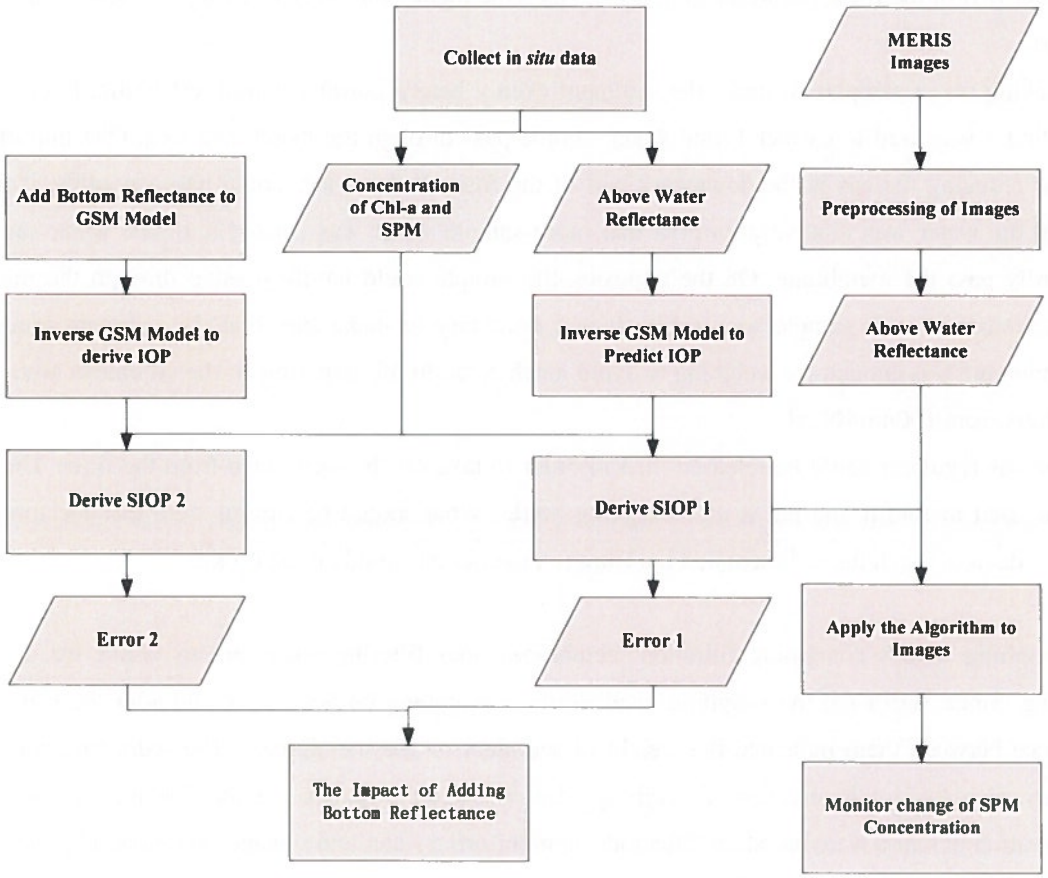

Figure5-1 Flowchart of research methodology

From figure5-1 we can conclude the methodology of this study into four steps: i) calibrating of GSM model; ii) adding of bottom reflectance; iii) analysis of adding bottom reflectance; iv) processing and analysis of images. These steps are all based on the field campaign which provides in situ data of remote sensing reflectance and concentration of SPM and Chl-a in Poyang Lake.

Step 1 Inverse GSM model

The empirical values (Maritorena et al. 2002) in GSM model were used. We inverted the remote sensing reflectance R_{rs} of part of the sample points to derive the the IOP. Using the derived IOP values and in situ measured concentrations we computed the SIOP of SPM and Chl-a in this lake

Step 2 Add bottom reflectance to the model

By adding the bottom reflectance factor to the GSM model, the retrieval products are IOP a(λ) and bb(λ) and the bottom reflectance RB when the inputs are remote sensing reflectance Rrs of part of sample points. In this research the bottom depth is set of 10 meters which is the average value of the sampling period(Center for Remote Sensing/GIS Application of Jiangxi Province 2003). Using the points from images, the average bottom reflectance can be calculated and divided by the reflectance value at 550nm which results in the normalized bottom reflectance. We assume that the normalized bottom reflectance represents the spectral shape of the whole lake's bed. In other words we reduced the unknown spectrum of bottom albedo to one value which is the bottom reflectance at 550nm. In this step, the derived IOP should be again used to calculate SIOP. Additionally, the uncertainties of this model can be obtained.

Step 3 Analysis of bottom reflectance impact

Then we can use the other part of in situ data to evaluate whether the model and the derived SIOP are reliable. After evaluation the errors of the model with and without the bottom reflectance we can compare the difference between them and discuss them.

Step 4 Image processing and application

After preprocessing of the images, we can apply the model to these images to inverse the map of concentration of suspended particles. By comparing the maps in the last three years within the same period of each year, we can easily explore the change of suspended particles in Poyang Lake.

Table 5-1 Software been used in this research

Software	Functions
Microsoft Excel 2003	Data processing
IDL 6.3	Image processing
Matlab 7.1	Model inversion
SPSS 13.0	Statistical analysis
BEAM 4.5	Image processing and application
Microsoft Word 2003	Word processing

5.2. Inverse GSM model

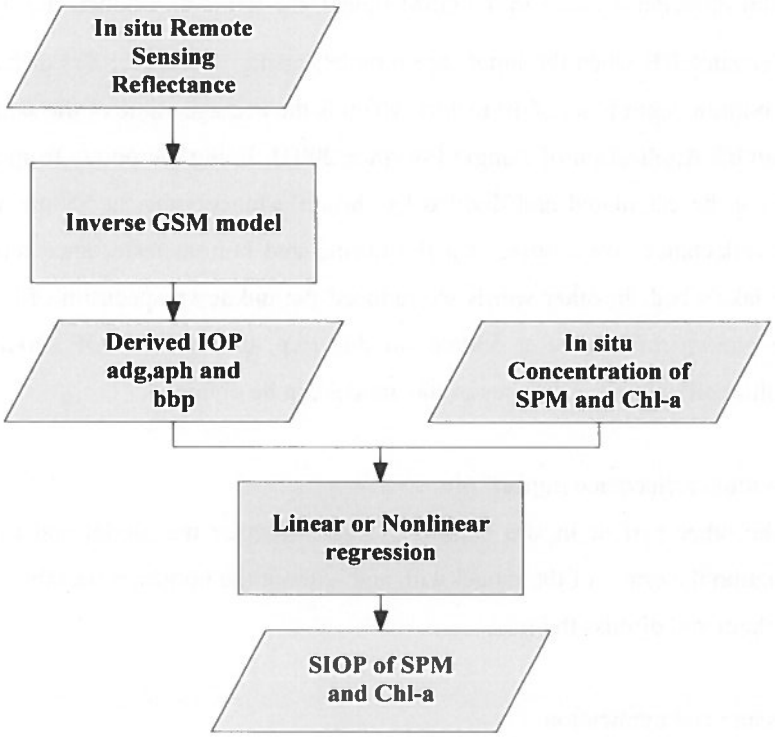

Figure 5-2 Flow chart on inverse GSM model

There is a relation between remote sensing reflectance and $b_b/(a+b_b)$ (Gordon et al. 1988). Here a represents the total absorption coefficient while b_b means the total backscattering coefficient. They are expressed as:

$$a(\lambda) = a_w(\lambda) + a_{dg}(\lambda) + a_{ph}(\lambda), \tag{5-1}$$

$$b_b(\lambda) = b_w(\lambda) + b_{bp}(\lambda), \tag{5-2}$$

The empirical values of water absorption and water backscattering are from the previous research (Smith and Baker 1981; Pope and Fry 1997). From the IOCCG report, the model is known as:

$$R_{rs,\infty}(\lambda) = \frac{t^2}{n_w^2} \sum_{i=1}^{2} g_i \left(\frac{b_b(\lambda)}{b_b(\lambda) + a(\lambda)}\right)^i, \quad (5\text{-}3)$$

The $R_{rs,\infty}$ here is the remote sensing reflectance for optically deep water. From the GSM model, g1 (=0.0949) and g2 (=0.0794) are geometrical factors and t and n_w are constant parameters that are calculated by a large *in situ* data set (Maritorena and Siegel 2006). t (=1.34) is the sea-air transmission factor and n_w (=1.33) is the index of refraction of the water (for details of these coefficients, see Maritorena and Siegel 2005).

$$a_{dg}(\lambda) = a_{dg}(\lambda_0)\exp(-S(\lambda - \lambda_0)), \quad (5\text{-}4)$$

$$b_{bp}(\lambda) = b_{bp}(\lambda_0)\left(\frac{\lambda_0}{\lambda}\right)^Y, \quad (5\text{-}5)$$

$$a_{ph}(\lambda) = a^*_{ph}(\lambda)C, \quad (5\text{-}6)$$

Here S is the spectral attenuation constant for the absorption coefficient of CDOM (Bricaud et al. 1981), and Y is the power law exponent for the backscattering coefficient of SPM (Lee et al. 1996). We define the slope of CDOM is 0.015 and exponent is 0.9. In Lee et al. (1999), the S was fixed as 0.015 and Y is in a range of 0 to 2.5 (Lee et al. 1999). By trying with different Y values, Y=0.9 gave the most suitable result in this case. Firstly, give a guess number which is from a large in situ data set and then apply a nonlinear least-square function to fit the equation that links remote sensing reflectance to IOP (equation5-3). By doing this we will get the IOP of $a_{dg}(440)$, C and $b_{bp}(440)$. From the equation 5-4, 5-5 and 5-6 the IOP in other wavelengths can be easily referred. And the absorption of Chl-a is then calculated by the equation 1.1 and the IOP of a_{dg} and b_{bp}.

Table 5-2 Empirical values for water absorption and backscattering

Wavelength	Water absorption	Water backscattering
410	0.00473	0.003416
440	0.00635	0.002517
490	0.015	0.001581
510	0.0325	0.00133
560	0.0619	0.000888

(Source: Smith and Baker 1981; Pope and Fry 1997)

Table 5-3 Empirical values for specific Chl-a absorption

Wavelength	a_{ph}*
410	0.00665
440	0.05582
490	0.02055
510	0.01910
560	0.01015

(Source: Maritorena et al. 2002)

The next step is using these retrieved IOP to calculate SIOP together with related measured concentration. In SPSS, we can use multiple regressions to search what the equation really is. There are many possibilities and, taken SPM for example, can be mainly concluded as:

$b_{bp} = \alpha C_{SPM} + \beta$, α and β are linear coefficients;

$b_{bp} = \alpha e^{\beta C_{SPM}}$, α and β are exponential coefficients;

$b_{bp} = \alpha \ln C_{SPM} + \beta$, α and β are logarithmic coefficients.

As in GSM model, we have derived IOP in five bands which are coordinating with the wavelengths in MERIS. Here we can calculate the SIOP in these bands to build the SIOP library for Poyang Lake. However, only the bands that show satisfactory results, which indicate less error in retrieving SIOP, are retained and used in further research.

5.3. Derive the uncertainties of the GSM model

From Maritorena and Siegel (2005), the quantification of confidence intervals, ci, can be identified as for the retrievals using a linear approximation to the calculation of nonlinear regression inference regions (Bates and Watts 1988). If Y is a vector of p retrieved products, then

$$ci(Y_p) = se\ (Y_p)t(n\text{-}p; \alpha/2), \tag{5-7}$$

In this expression, se (Y_p) is the standard error of the pth estimates of Y while $t(n\text{-}p; \alpha/2)$ represents the upper $\alpha/2$ quantile for the retrieved products' n-p degrees' freedom.

5.4. Adding bottom reflectance to GSM model

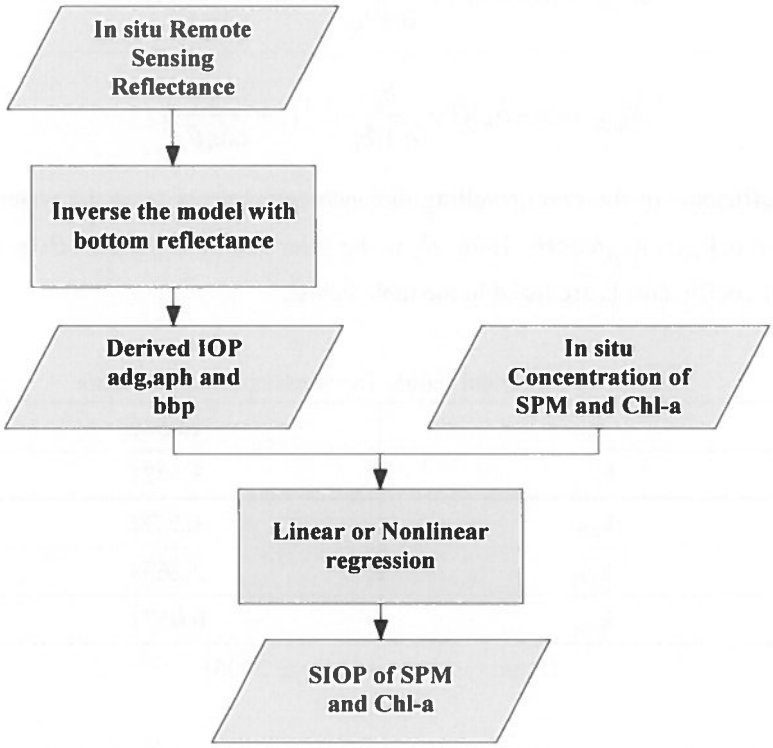

Figure 5-3 Flowchart on adding bottom reflectance

When the above surface signals are measured by a sensor, these signals conclude three parts which are the reflected skylight, the path radiance of water column and the bottom reflectance (Lee et al. 1998). For shallow waters, the bottom reflectance is significant thus should be taken into consideration when retrieving IOP.

Albert and Mobley (2003) have developed parameterizations of R and R_{rs} for shallow case-2 waters. To add the bottom reflectance impact to the GSM model, the equation is given as below(Albert and Gege 2006):

$$R_{rs} = R_{rs,\infty}\{1 - A_{rs,1}\exp[-(K_d + k_{u,W})z_B\} + A_{rs,2}\frac{R_B}{\pi}\exp[-(K_d + k_{u,B})z_B]., \quad (5\text{-}8)$$

Here, $R_{rs,\infty}$ represents the remote sensing reflectance for optically deep water which is presented in the same way as for the GSM model. The R_{rs} is the measured remote sensing reflectance for shallow waters. The empirical coefficients of $A_{rs,i}$ have been set and the downward and upward diffuse attenuation coefficients K_d, $K_{u,W}$ and $K_{u,B}$ can be calculated from IOP. For shallow water, $A_{rs,1}$=1.1576 and $A_{rs,2}$=1.0389.

$$K_d = k_0\frac{a + b_b}{\cos\theta_s}, \quad (5\text{-}9)$$

$$K_{u,W} = (a+b_b)(1+\frac{b_b}{a+b_b})^{k_{1,W}}(1+\frac{k_{2,W}}{\cos\theta_s}), \quad (5\text{-}10)$$

$$K_{u,B} = (a+b_b)(1+\frac{b_b}{a+b_b})^{k_{1,B}}(1+\frac{k_{2,B}}{\cos\theta_s}), \quad (5\text{-}11)$$

The attenuation coefficients of the two upwelling radiance components from the water is $k_{u,W}=K_{u,W}/\cos\theta_v$ and from the bottom is $k_{u,B} = K_{u,B}/\cos\theta_v$. Here θ_s is the solar zenith angle and θ_v is the viewing azimuth angle. The values of coefficients k_i are listed in the table below.

Table 5-4 Empirical values for attenuation coefficients

k_0	1.0546
$k_{1,W}$	3.5421
$k_{2,W}$	-0.2786
$k_{1,B}$	2.2658
$k_{2,B}$	0.0577

(Source: Albert and Gege 2006)

For the parameterization, the same methods are conducted as in the GSM model. The detritus and glebstoff absorption $a_{dg}(\lambda) = a_{dg}(440)\exp(-S(\lambda-440))$ while S=0.015. The particles backscattering coeffient $b_{bp}(\lambda) = b_{bp}(440)(\frac{440}{\lambda})^Y$ and Y=0.9. And $a_{ph}(\lambda) = a^*_{ph}(\lambda)\cdot C_{Chl-a}$ with the empirical a_{ph}* values listed in table 5-3.

The parameterization of bottom albedo is also needed for inversion of the model. According to Lee's research (1998), $R_B(\lambda) = R_B(550)\rho(\lambda)$ and the $\rho(\lambda)$ is the 550nm normalized albedo shape which is based on sandy bottom (Lee et al. 1998). In this research, the 550nm normalized albedo is derived from the image. As in the field days, it was during the transition period from wet to dry season and in some places the bottom was above water surface therefore the bottom reflectance can be directly obtained from the images.

The steps on calculating normalized bottom albedo are as followed. Firstly the images should be preprocessed to provide reliable reflectance and the preprocessing methods are introduced in the next section so that we would not discuss it here. Then from the comparison with images of the same period but from other sources we can have a basic knowledge on the areas that are inclined to be sandy bottom but not water. To make sure that the area been chosen is bottom but not water, we could not just rely on experiences because the water conditions differ a lot. A more scientific way is thus conducted which is the comparison of the spectral shape between the selected area and water. As we know the water spectral shape is specific and

easily to distinguish from sand. When the bottom area has been determined, six points are used to calculate the average reflectance of these points. Then the reflectance in each band is divided by that in 550nm which produce the result of $\rho(\lambda)$. In this research, we choose 560nm of MERIS band to do the calculation because this band in MERIS is most close to the wavelength of 550nm.

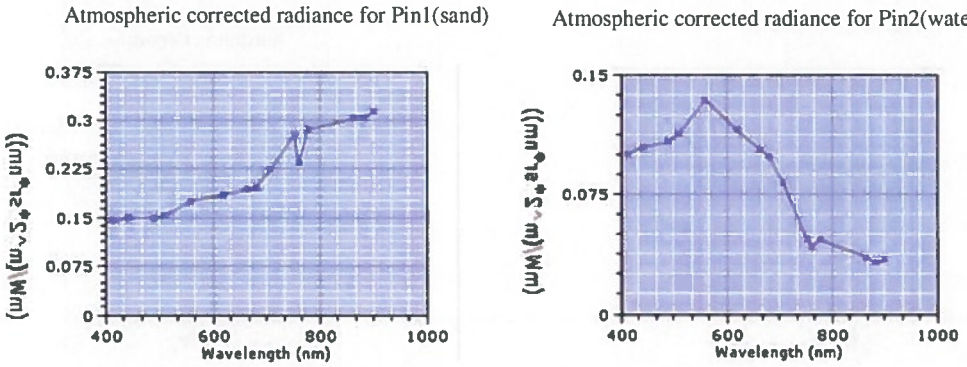

Figure 5-4 spectral shape of sand and water

Figure 5-4 shows the spectra shape of sand and water respectively. Form them the non-water area in the main lake can be told from water. The sand spectrum comes from pin1 and pin2 is in water area.

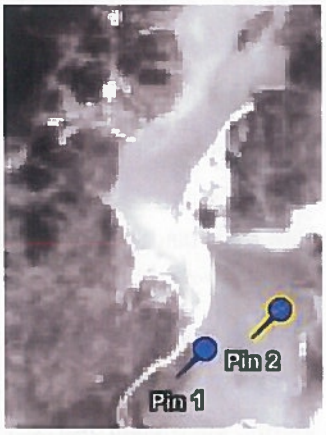

Figure 5-5 Locations of Pins on finding bottom area based on spectral shape

Since in the assumption, one bottom type is assumed; the bottom have the same spectral shape. As a result, six points around this pin1 (include pin1) who have similar spectrum were chosen and the average remote sensing reflectance is measured. After divided by the reflectance in 560, the normalized bottom albedo is determined.

Table5-5 Normalized bottom albedo

Wavelength	410	440	490	510	560	620	660	680	710
$\rho(\lambda)$	0.8306	0.8571	0.8509	0.8695	1	1.0576	1.10456	1.1218	1.2805

5.5. Validation of GSM model and adding bottom reflectance model

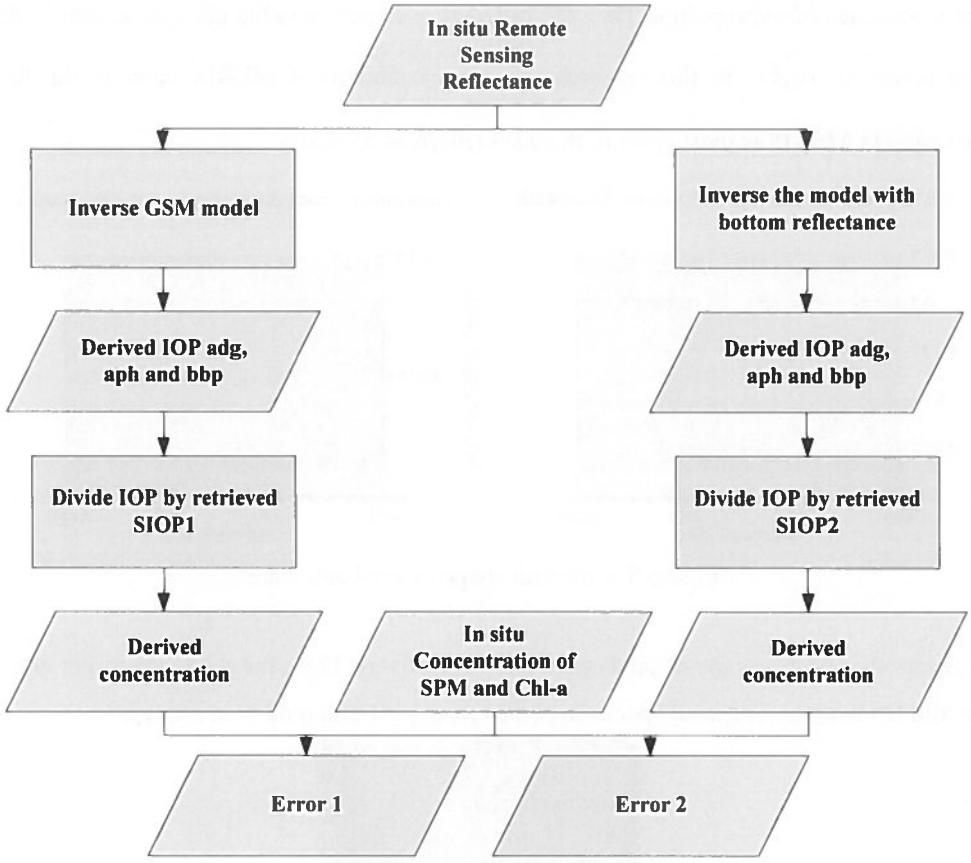

Figure5-6 Flowchart on validation

To analyze the impact of adding the bottom reflectance to the model, the validation of the models with and without bottom effect should be conducted first. The other half of in situ samples are used here since the former half are used in inversion IOP and calculating SIOP.

(1) Applying the measured reflectance to inverse the GSM model again to retrieve IOP of Chl-a absorption coefficient a_{ph} and particles backscattering coefficient b_{bp}. When the IOP are obtained, the SIOP that retrieved from 5.2 are used as division. The results of this calculation are concentrations of SPM and Chl-a.

(2) Meantime inverse the model that includes bottom reflectance to derive IOP as well. In this case, the SIOP from 5.3 should be taken to conduct the calculation of concentration.

(3) For both concentrations of water composition that calculated from the above steps, the in situ concentrations are used to validate them. In a perfect situation, the derived concentrations will be equal to the measured ones but in actual, there are always errors between them. The errors from the GSM model without and with bottom reflectance are named error 1and error 2 respectively.

(4) The comparison of error 1 and error 2 can to some extent tell the impact of adding bottom reflectance to the GSM model.

5.6. Image processing

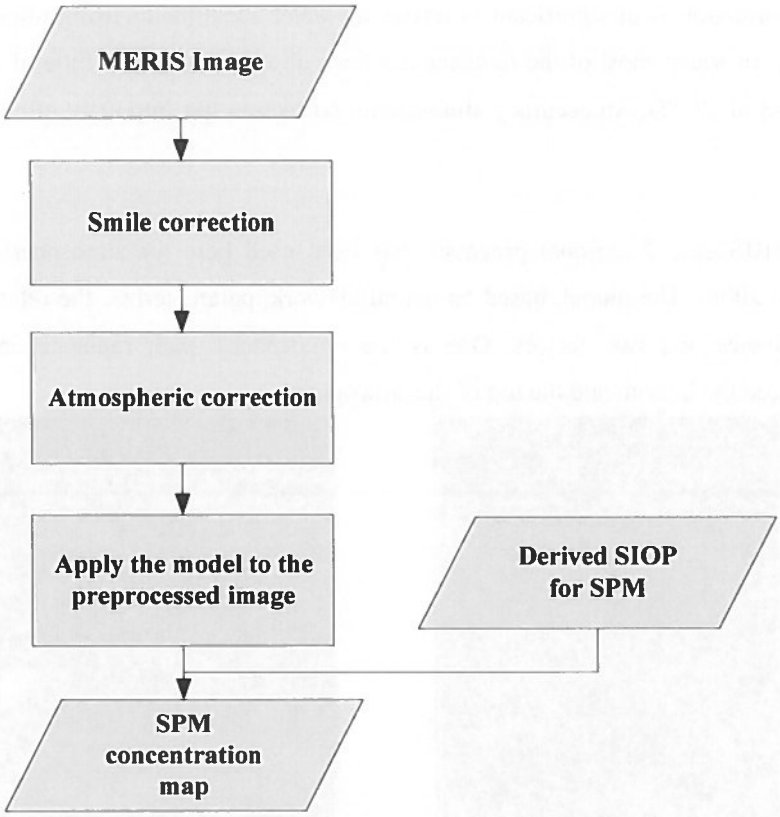

Figure5-7 Flowchart on image processing

5.6.1. Image smile correction

As the CCD technique is used in MERIS which leads to variations of the spectral wavelength, the images should be processed by smile correction. This so called smile effects come from the variation of the spectral wavelength at every pixel because CCD measurement measure in one dimension on one image line and disperse radiance for every pixel in the other dimension. The variation here is small compared with the bandwidth in MERIS but we still should take it into consideration as retrieval of the IOP in water requires high accuracy.

The level 2 products in MERIS have included the result of smile correction but since what we are using in this research is level 1b products which giving the direct measuring result of radiance, the smile correction is carried out.

There are two terms in smile correction which are the irradiance correction and the reflectance correction. The objective of irradiance correction is correcting the difference of the solar irradiance and for reflectance correction it is interpolating the slope of reflectance from pixel to the reference wavelength. The smile correction is the sum of them.

5.6.2. Atmospheric correction

The atmospheric correction is of significant in retrieving water constituents using remote sensing methods (Pietro et al. 2001). In water, most of the radiance has been absorbed and only little of them can be used in the retrieval(Chen et al. 2007). An accuracy atmospheric correction has important effect on the accuracy of the result.

A plug-in, the MERIS case 2 regional processor has been used here for atmospheric correction(BEAM Development Team 2008). The model, based on neural network, parameterizes the relation between the top of atmosphere radiance and two factors. One is the atmospheric path radiance and the other is the transmittance between the bottom and the top of the atmosphere.

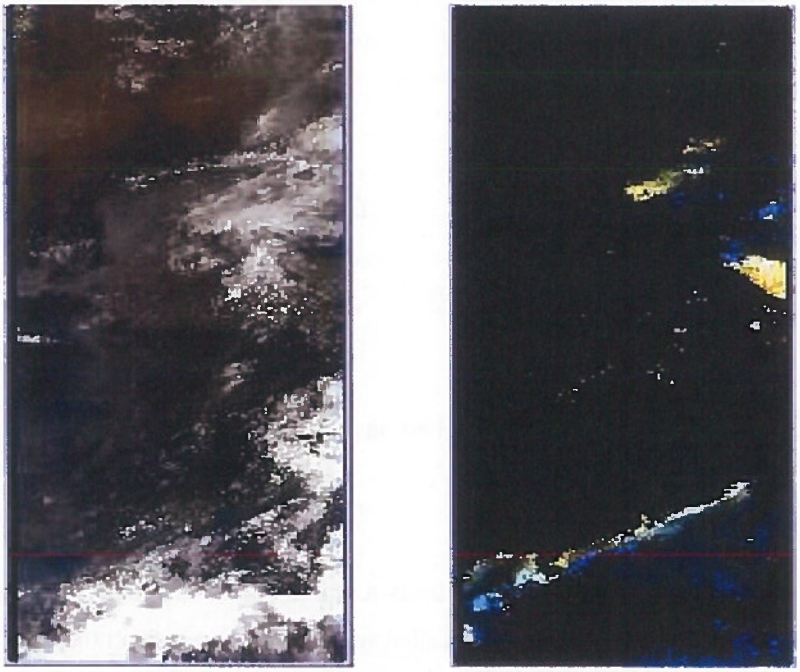

Figure 5-8 RGB images of before and after atmospheric correction

5.6.3. Subset of images

The MERIS image is so large that it covers an area which is much more than the study area. Before applying the algorithm to the image, it should be subset to a smaller size to improve the calculating speed. In the output of atmospheric correction, the image contains all the atmospheric parameters which we do not need in the next steps. We remain only the water leaving reflectance of the first five bands in MERIS which are the bands we need for the model.

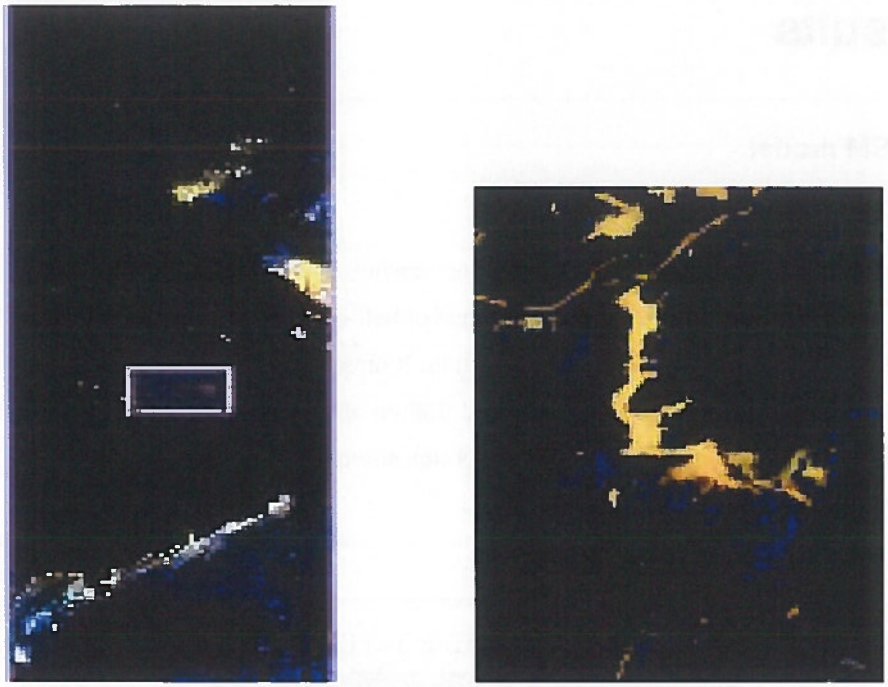

Figure 5-9 Subset of image

5.6.4. Apply the algorithm to the image

The algorithm of the relation between backscattering coefficient of SPM and the concentration of SPM was then applied to the image. Two methods were used here to retrieve the backscattering coefficient map. As the GSM model was applied and validated in the previous steps, the model can be applied to the whole image pixel by pixel using IDL. The other method was directly using the MERIS case 2 regional processor in the same way as has been done in the atmospheric correction to retrieve the IOP of the lake. This method, as illustrated in the upper section, uses a neural network to retrieve the atmospheric parameters as well as the IOP and water component.

In BEAM, a simple threshold was put on this backscattering coefficient to mask the area not belonged to Poyang Lake. If b_{bp} is more than 0, then show the value of b_{bp} otherwise give no-data to the pixel.
The SIOP that has less error in the above sections was used here to retrieve SPM concentration by b_{bp}. The band arithmetic in BEAM executed the calculation. Additionally, the color legend was added to the achieved map from which we can easily explore the spatial variation of SPM concentration.

6. Results

6.1. For GSM model

6.1.1. Results on inverse GSM model

After the filed work we have obtained the remote sensing reflectance of water samples from the ASD spectrometer. Figure6-1 shows the average reflectance of half of the water samples which includes 15 points. The other half of these samples was used for validation. It presents a typical remote sensing reflectance trend of water by high reflectance at wavelength around 560nm and 680nm and reaches the higher peak at the wavelength of 560nm. The locations and the water composition concentration are listed in the Appendix A, B and C.

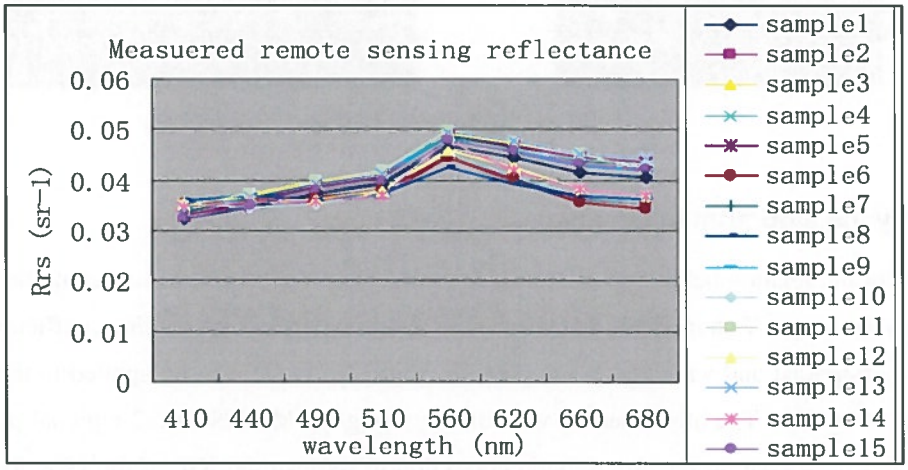

Figure 6-1 Measured R_{rs} of water samples

When applying this reflectance into GSM model, the outputs are backscattering coefficient of SPM (b_{bp}), the absorption coefficient of CDOM (a_{dg}) and the absorption coefficient of Chl-a (a_{ph}). Table 6-1 gave the retrieved IOP values in detail at the wavelength of 440nm. The values at other bands can be calculated by the spectral relation illustrated in Chapter 5. Since the concentration of CDOM was not measured in this research, the absorption coefficient of CDOM will not be discussed furthermore.

Table 6-1 Retrieved IOP values

Sample No.	bbp(440) (m^{-1})	aph(440) (m^{-1})	adg(440) (m^{-1})
1	0.068118	0.107213	0.11736
2	0.070869	0.108335	0.1209
3	0.062515	0.097171	0.094914
4	0.051083	0.059314	0.083512
5	0.086706	0.167053	0.13082
6	0.071971	0.115782	0.11354
7	0.067436	0.103753	0.11427
8	0.081883	0.144295	0.12979
9	0.071459	0.111807	0.11773
10	0.065451	0.104958	0.1119
11	0.07771	0.11452	0.12193
12	0.079968	0.125048	0.12376
13	0.07738	0.122307	0.12249
14	0.073622	0.117992	0.11422
15	0.075434	0.121961	0.11473

6.1.2. Results on calculating SIOP

Calculated by the retrieved IOP and the in situ concentrations of SPM and Chl-a of these samples, the results of possible SIOP, the R square and RMSE at 440nm are shown below.

- For b_{bp}*

Table6-2 R^2 and RMSE of three regression methods on calculating b_{bp}*

Regression methods	Linear	Logarithmic	Exponential
R^2	0.853	0.864	0.825
RMSE	0.731	0.635	0.910

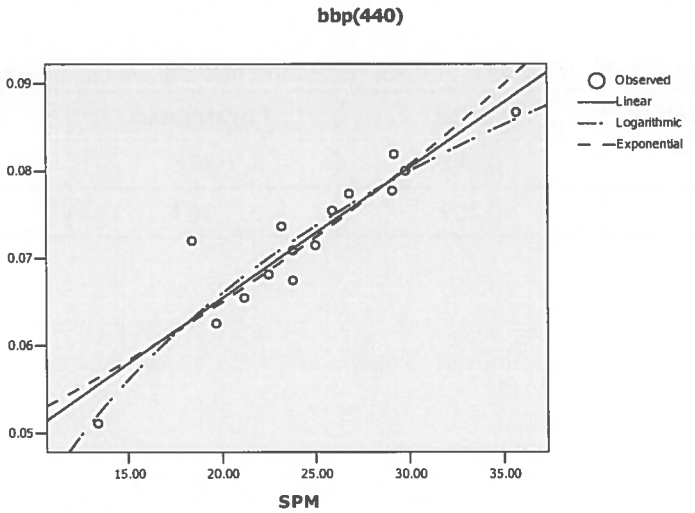

Figure 6-2 Relation between measured SPM concentration and retrieved b_{bp}

Table6-2 gives us information on the R^2 of Linear, Logarithmic and Exponential regression methods at the first five bands of MERIS. As we have inferred from the parameterization method, the R^2 are the same at each band. But it differs at these three regression methods. The RMSE differs slightly between these bands and the RMSE at 440nm is chosen here. The error indicates that the retrieved backscattering coefficient has a strong relation with the in situ concentration of SPM using all of these regression methods while the logarithmic way is the best and linear way appears good as well. However in this regression, we choose only 15 samples so that the logarithmic way may not be the most appropriate one and we will remain the linear way as well in the validation.

Table6-3 provides the coefficients of the linear regression. In the linear regression, the slopes have little difference ranging from 0.0012 to 0.0016 and the intercepts range from 0.0286 to 0.0378. The equations are given in a format of $b_{bp} = \alpha\ C_{SPM} + \beta$, while α and β are the calculated coefficients which are also considered as SIOP.

Table 6-3 Coefficients of linear regression on calculating b_{bp}*

MERIS Bands(nm)	Intercept	Slope	Equations
410	0.0378	0.0016	b_{bp} =0.0016 C_{SPM} +0.0378
440	0.0355	0.0015	b_{bp} =0.0015 C_{SPM} +0.0355
490	0.0322	0.0014	b_{bp} =0.0014 C_{SPM} +0.0322
510	0.029	0.0012	b_{bp} =0.0012 C_{SPM} +0.029
560	0.0286	0.0012	b_{bp} =0.0012 C_{SPM} +0.0286

- For a_{ph}*

The R^2 in the deriving of absorption coefficient of Chl-a is much lower compared with SPM but still reliable enough to retrieving SIOP. The differences between these three retrieval methods are slight and the linear way has the lowest RMSE.

Table 6-4 R^2 and RMSE of three regression methods on calculating a_{ph}*

Regression method	Linear	Logarithmic	Exponential
R^2	0.685	0.676	0.680
RMSE	0.209	1.163	3.227

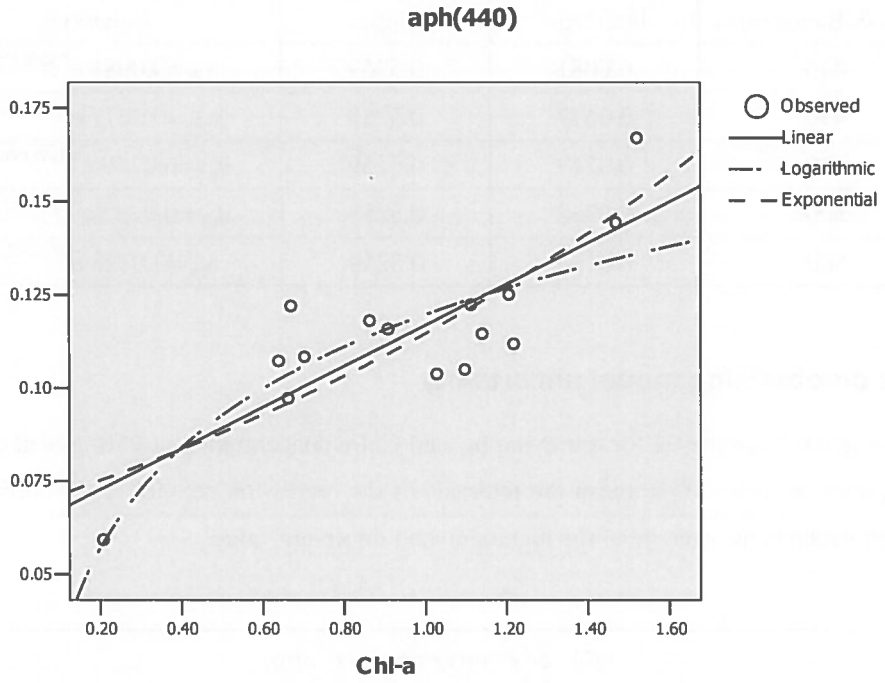

Figure 6-3 Relation between measured Chl-a concentration and retrieved a_{ph}

Tables 6-5, 6-6 and 6-7 are the deriving SIOP for Chl-a from linear, logarithm and exponential methods respectively.

Table 6-5 Coefficients of linear regression on calculating a_{ph}*

MERIS Bands (nm)	Intercepts	Slopes	Equations
410	0.0074	0.0066	a_{ph} =0.0066 C_{chl-a} +0.0074
440	0.0617	0.0551	a_{ph} =0.0551 C_{chl-a} +0.0617
490	0.0227	0.0203	a_{ph} =0.0203 C_{chl-a} +0.0277
510	0.0211	0.0188	a_{ph} =0.0188 C_{chl-a} +0.0211
560	0.0112	0.01	a_{ph} =0.01 C_{chl-a} +0.0112

Table 6-6 Coefficients of logarithm regression on calculating a_{ph}*

MERIS Bands (nm)	Intercepts	Slopes	Equations
410	0.0143	0.0046	a_{ph} =0.0046Ln(C_{chl-a})+0.0143
440	0.1197	0.0389	a_{ph} =0.0389Ln(C_{chl-a})+0.1197
490	0.0441	0.0143	a_{ph} =0.0143Ln(C_{chl-a})+0.0441
510	0.0409	0.0133	a_{ph} =0.0133Ln(C_{chl-a})+0.0409
560	0.0218	0.007	a_{ph} =0.0071Ln(C_{chl-a})+0.0218

Table 6-7 Coefficients of exponential regression on calculating a_{ph}*

MERIS Bands (nm)	Intercepts	Slopes	Equations
410	0.0081	0.5259	$a_{ph}=0.0081\ e^{0.5259\ Cchl\text{-}a}$
440	0.0677	0.5259	$a_{ph}=0.0677\ e^{0.5259\ Cchl\text{-}a}$
490	0.0249	0.5259	$a_{ph}=0.0249\ e^{0.5259\ Cchl\text{-}a}$ 7
510	0.0232	0.5259	$a_{ph}=0.0232\ e^{0.5259\ Cchl\text{-}a}$ 1
560	0.0123	0.5259	$a_{ph}=0.0123\ e^{0.5259\ Cchl\text{-}a}$

6.2. Results on obtaining model uncertainty

The figures 6-4 and 6-5 are the CI for retrieving b_{bp} and Chl-a concentration at 95% global confidence. The red and blue points at each sample mean the intervals of the regression activity. The yellow points are the retrieving result which is the average of the maximum and minimum value.

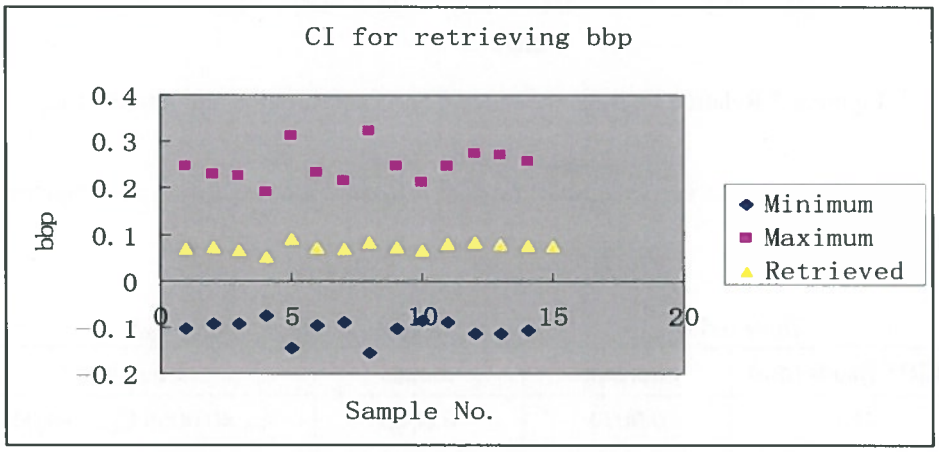

Figure 6-4 CI for retrieving bbp

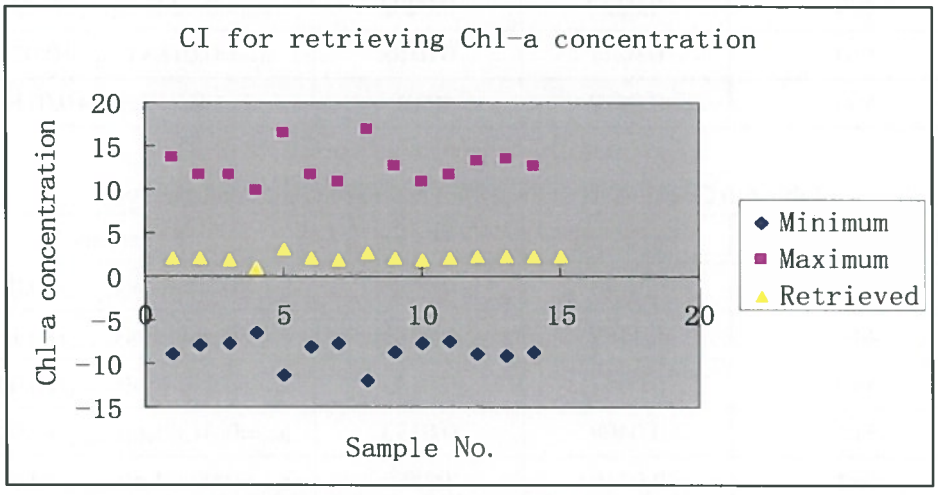

Figure 6-5 CI for retrieving Chl-a concentration

6.3. Results on inverse GSM model within adding bottom reflectance

6.3.1. Results on model inversion

When inverse the GSM model within bottom reflectance, the outputs contains the backscattering coefficient of SPM, the absorption coefficient of Chl-a and CDOM and the bottom reflectance. As it used the same way to parameterize the aph and bbp, they have the same spectral relation in every band as in GSM model. But compared with the results in GSM inversion, they are relatively lower in value because the remote sensing reflectance above water is not only affected by water composition but also by bottom reflectance.

Table 6-8 Retrieved IOP and bottom reflectance values

Sample No.	bbp(440)(m^{-1})	aph(440)(m^{-1})	adg(440)(m^{-1})	RB(550)(sr^{-1})
1	0.00118	0.002012	0.018638	0.068041
2	0.00093	0.002181	0.017261	0.068929
3	0.00088	0.002371	0.018616	0.069461
4	0.00056	0.001565	0.019382	0.065008
5	0.00188	0.002571	0.016786	0.070579
6	0.00069	0.00226	0.017036	0.07003
7	0.00111	0.00209	0.016666	0.067266
8	0.00268	0.002432	0.012866	0.067266
9	0.00102	0.002482	0.012321	0.069329
10	0.00109	0.003132	0.010064	0.065756
11	0.00198	0.00324	0.01225	0.071823
12	0.00144	0.002125	0.012261	0.071981
13	0.00128	0.002095	0.014425	0.070731
14	0.000881	0.002363	0.012521	0.070834
15	0.00105	0.002363	0.012342	0.071524

6.3.2. Results on calculating SIOP

- For b_{bp}*

Then, the SIOP of b_{bp}* has been calculated using the retrieved b_{bp} and the in situ concentration again with these regression method. In this model, table 6-9 shows that the R^2 in calculating SIOP is not as good as that in GSM model and the RMSE is relatively higher. Both the linear and the exponential method are taken into consideration in the following steps.

Table 6-9 R^2 and RMSE of three regression methods on calculating b_{bp}*

Regression method	Linear	Logarithmic	Exponential
R^2	0.590	0.525	0.737
RMSE	3.660	7.319	3.616

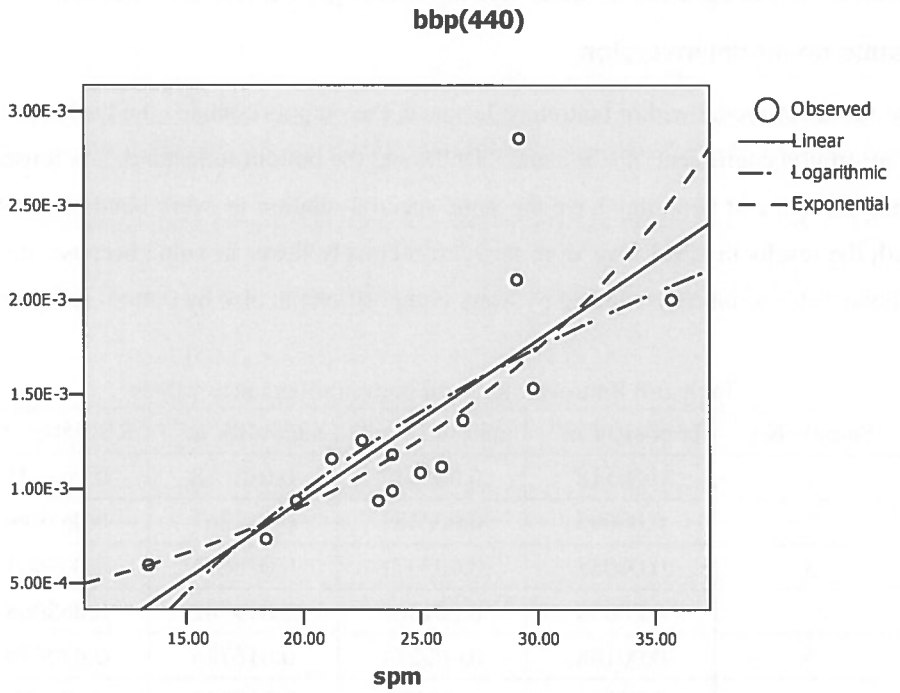

Figure 6-6 Relation between measured SPM concentration and retrieved b_{bp}

Table 6-10 and 6-11 are the coefficients of calculating SIOP for SPM. In the linear way, the values of intercepts and slopes are very small considered a small backscattering coefficient value. In the exponential way, the values of intercepts and slopes are all the same in these bands. This indicates a small variation of retrieved IOP in each wavelength.

Table 6-10 Coefficients of the linear regression on calculating b_{bp}*

MERIS Bands (nm)	Intercepts	Slopes	Equations
410	-0.0007	0.00008	$b_{bp}=0.00008C_{SPM}-0.0007$
440	-0.0007	0.00008	$b_{bp}=0.00008C_{SPM}-0.0007$
490	-0.0006	0.00007	$b_{bp}=0.00007C_{SPM}-0.0006$
510	-0.0006	0.00007	$b_{bp}=0.00007C_{SPM}-0.0006$
560	-0.0006	0.00006	$b_{bp}=0.00006C_{SPM}-0.0006$

Table 6-11 Coefficients of the exponential regression on calculating b_{bp}*

MERIS Bands (nm)	Intercepts	Slopes	Equations
410	0.0002	0.0648	$b_{bp}=0.0002\ e^{0.0648CSPM}$
440	0.0002	0.0648	$b_{bp}=0.0002\ e^{0.0648CSPM}$
490	0.0002	0.0648	$b_{bp}=0.0002\ e^{0.0648CSPM}$
510	0.0002	0.0648	$b_{bp}=0.0002\ e^{0.0648CSPM}$
560	0.0002	0.0648	$b_{bp}=0.0002\ e^{0.0648CSPM}$

- For a_{ph}*

The R^2 of these regression method on calculating a_{ph}* is so low that the retrieved absorption coefficient of Chl-a is inappropriate to be applied in deriving SIOP here. In all these three ways, table 6-12 shows that the R^2 is less than 0.4 and the RMSE is more than 3. Figure6-7 describes the relation between the regression line and the Chl-a concentration. Many points are far from the proposed relation, which leads to the low R^2 and high RMSE.

Table 6-12 R^2 of three regression methods on calculating a_{ph}*

Regression method	Linear	Logarithmic	Exponential
R^2	0.288	0.356	0.345
RMSE	3.350	7.933	7.683

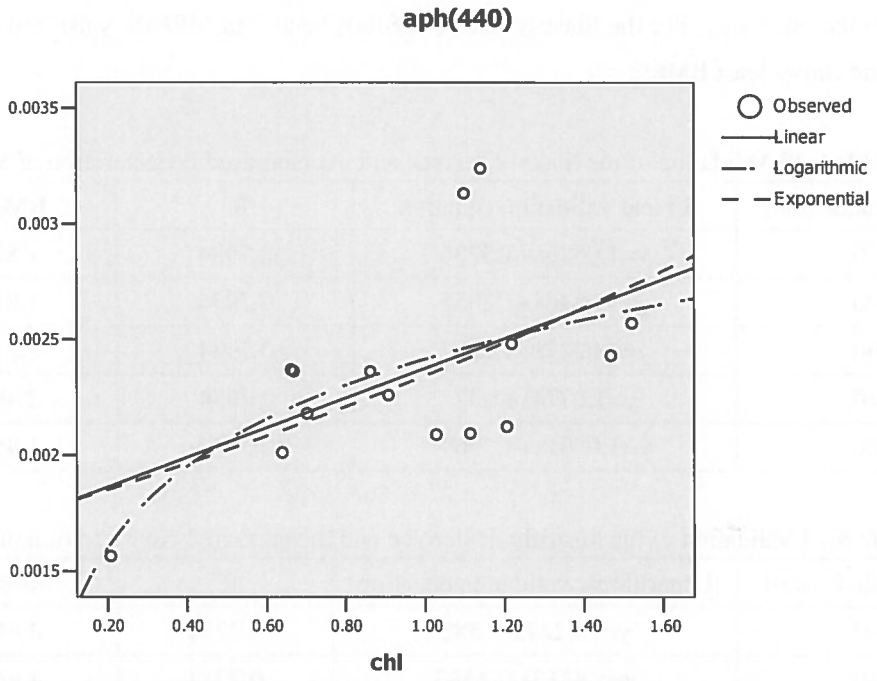

Figure 6-7 Relation between measured Chl-a concentration and retrieved a_{ph}

6.4. Validation of the models and the analysis of adding bottom reflectance

The other fifteen samples are used to inverse IOP in both GSM model and the model with bottom reflectance. In this section, the models are validated by comparing the in situ concentration of SPM and Chl-a with the deriving concentrations of them. The deriving concentrations are calculated by the IOP of these fifteen samples and the retrieved SIOP in section 6.1 and 6.3.

6.4.1. Validating GSM model

The in situ concentration and the calculated concentration are compared to validate both the model itself and the retrieved SIOP. In a perfect situation, y=x while y is the derived and x is the measured concentration. As in the retrieving of SIOP for backscattering coefficient of SPM in 6.1, the R^2 is more than 0.8 and the RMSE is less than 0.8 which indicated less error in both linear and the logarithmic ways, both methods are validated here. And the derived concentration of Chl-a is calculated by all the three regression methods retrieved SIOP in section 6.1.

- For b_{bp}*

Tables 6-13 and 6-14 present the result of validating the GSM model and the retrieved SIOP. The equations mean the relation between the derived and the measured concentration. For both linearly and logarithmically retrieval method, the validation provides high R^2 although the linear way is a bit higher. But as the ideal result is y=x, the linear way is more close because the slops are around 1 and the intercepts are near 0 compared with the other way. For the linearly retrieved SIOP, band 3 in MERIS is the best which is mostly close to y=x and shows least RMSE.

Table 6-13 Validation of the linearly derived and the measured concentration of SPM

MERIS Bands (nm)	Linear validation equation	R^2	RMSE
410	y=1.0526x+1.3236	0.7934	1.801
440	y=1.0536x+1.3056	0.7934	1.812
490	y=1.0247x+1.2867	0.7934	1.217
510	y=1.0774x+1.37	0.7934	2.492
560	y=1.0601x+1.2969	0.7934	1.956

Table 6-14 Validation of the logarithmic derived and the measured concentration of SPM

MERIS Bands (nm)	Logarithmic validation equation	R^2	RMSE
410	y=1.4227x-7.582	0.7734	4.412
440	y=1.4313x-7.6583	0.7734	4.646
490	y=1.4326x-7.6798	0.7734	4.669
510	y=1.4376x-7.7173	0.7734	4.820
560	y=1.425x-7.59	0.7734	4.489

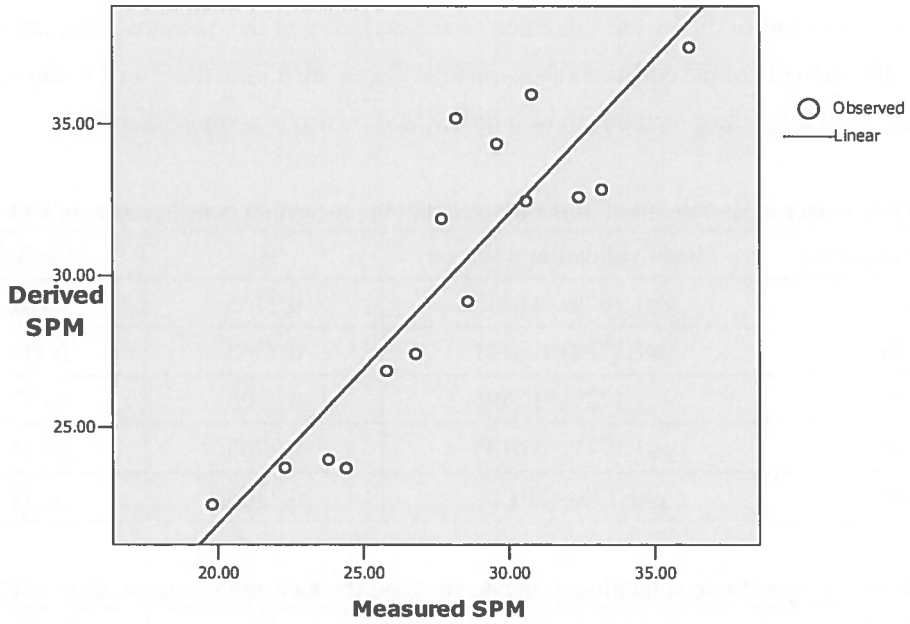

Figure 6-8 Comparison of derived and measured SPM

Figure 6-8 shows the values of the derived and the measured SPM concentration of linear retrieving method at 490nm. For these fifteen validating samples, most of them are well fit the regression line. To give more specific information on this figure, the values of this measured and derived SPM concentration are provided in table 6-15. The relative error is also calculated using a simple function of: Relative Error=100*(1-Derived/Measured) to show how the derived concentration fit the measured one.

Table6-15 Values of Measured and Derived SPM concentration and relative errors

Sample No.	Measured SPM(mg/L)	Derived SPM(mg/L)	Relative Errors
16	27.7	31.874	-15.068
17	30.8	35.974	-16.798
18	28.2	35.19	-24.787
19	29.6	34.34	-16.013
20	30.6	32.46	-6.078
21	33.2	32.842	1.078
22	36.2	37.525	-3.66
23	32.4	32.582	-0.561
24	28.6	29.15	-1.92
25	26.8	27.413	-2.287
26	24.4	23.644	3.098
27	23.8	23.926	-0.529
28	25.8	26.852	-4.077
29	22.3	23.653	-6.067
30	19.8	22.43	-13.282

- For a_{ph}*

From table 6-17 ,6-18 and 6-19, for the validation of the derived and the measured concentration of Chl-a, the R^2 is also high enough but the equations show that the slopes are a little far from 1 compared with that in SPM. However, all of these three methods show a little RMSE which is no more than 0.2.

Table 6-16 Linear validation of the derived and the measured concentration of Chl-a

MERIS Bands (nm)	Linear validation equation	R^2	RMSE
410	y=1.1674x-0.0215	0.7765	0.098
440	y=1.1738x-0.0141	0.7765	0.114
490	y=1.1729x-0.2596	0.7765	0.077
510	y=1.1771x-0.0135	0.7765	0.118
560	y=1.176x-0.0122	0.7765	0.119

Table 6-17 Logarithmic validation of the derived and the measured concentration of Chl-a

MERIS Bands (nm)	Logarithm validation equation	R^2	RMSE
410	y=1.6168x-0.4516	0.7493	0.124
440	y=1.6189x-0.445	0.7496	0.132
490	y=1.6176x-0.446	0.7495	0.129
510	y=1.6051x-0.4376	0.7495	0.137
560	y=1.176x-0.0122	0.7497	0.125

Table 6-18 Exponential validation of the derived and the measured concentration of Chl-a

MERIS Bands (nm)	Exponential validation equation	R^2	RMSE
410	y=1.0464x+0.1192	0.7786	0.133
440	y=1.0464x+0.1274	0.7786	0.144
490	y=1.0464x+0.1292	0.7786	0.147
510	y=1.0464x+0.1245	0.7786	0.140
560	y=1.0464x+0.129	0.7786	0.147

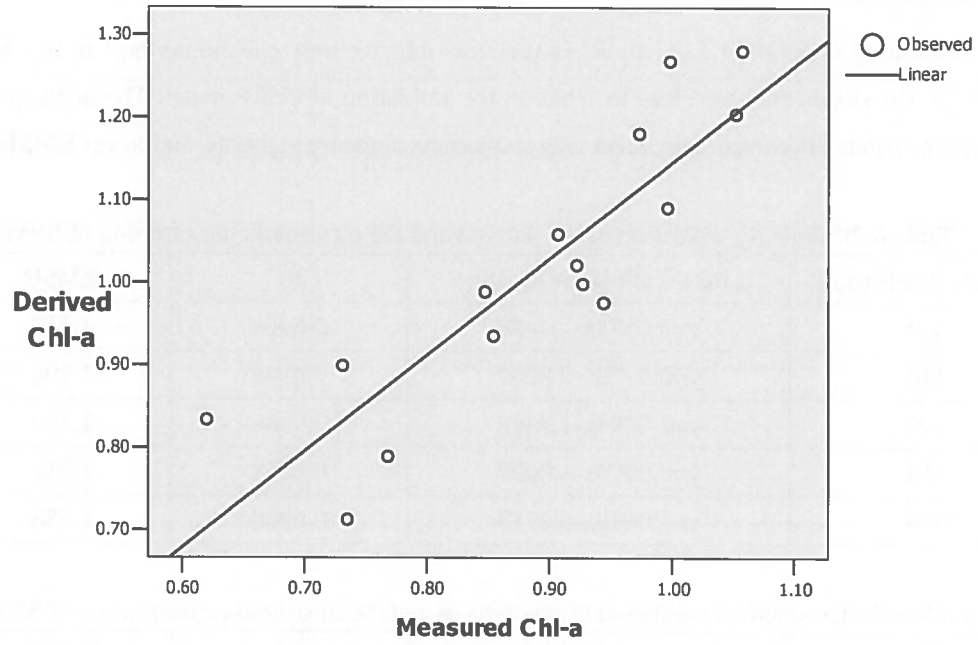

Figure 6-9 Comparison of derived and the measured Chl-a

Figure6-9, based on the linearly retrieved Chl-a concentration at 410nm, shows that the there is some difference between the derived and the measured Chl-a concentration. The values of them are listed in table 6-19. The relative errors are big which means the difference between them is obvious.

Table 6-19 Values of Measured and Derived Chl-a concentration and relative errors

Sample No.	Measured Chl-a(mg/m^3)	Derived Chl-a(mg/m^3)	Relative Errors
16	0.998	1.268	-27.054
17	0.973	1.18	-21.274
18	0.996	1.091	-9.538
19	0.907	1.058	-16.648
20	0.922	1.021	-10.737
21	0.735	0.712	3.129
22	1.052	1.204	-14.448
23	0.927	0.998	-7.659
24	0.847	0.989	-16.765
25	0.944	0.976	-3.389
26	0.854	0.935	-9.484
27	0.731	0.899	-22.982
28	1.057	1.28	-21.097
29	0.62	0.833	-34.354
30	0.768	0.789	-2.734

6.4.2. Validating GSM model within adding bottom reflectance

As in the calculating of SIOP of a_{ph}*, the R^2 is very low thus we only calculating b_{bp}* in 6.3. Herein table 6-20 and 6-21, the slopes are very close to 1 like in the validation of GSM model. The intercepts vary a lot according to the bands difference. The linear way shows advantage by higher R^2 and lower RMSE.

Table 6-20 Linearly validation of the derived and the measured concentration of SPM

MERIS Bands (nm)	Linear validation equation	R^2	RMSE
410	y=1.0573x-1.4489	0.6968	1.212
440	y=0.9922x-0.8209	0.6968	1.206
490	y=1.0293x-1.3568	0.6968	1.180
510	y=0.9929x-1.0057	0.6968	1.259
560	y=1.0649x-0.2713	0.6968	1.558

Table 6-21 Exponential validation of the derived and the measured concentration of SPM

MERIS Bands (nm)	Exponential validation equation	R^2	RMSE
410	y=0.9877x+3.1379	0.5462	3.080
440	y=0.9877x+2.1571	0.5462	2.455
490	y=9877x+0.6622	0.5462	2.015
510	y=0.9877x+0.1066	0.5462	2.009
560	y=0.9877x-1.1924	0.5462	2.328

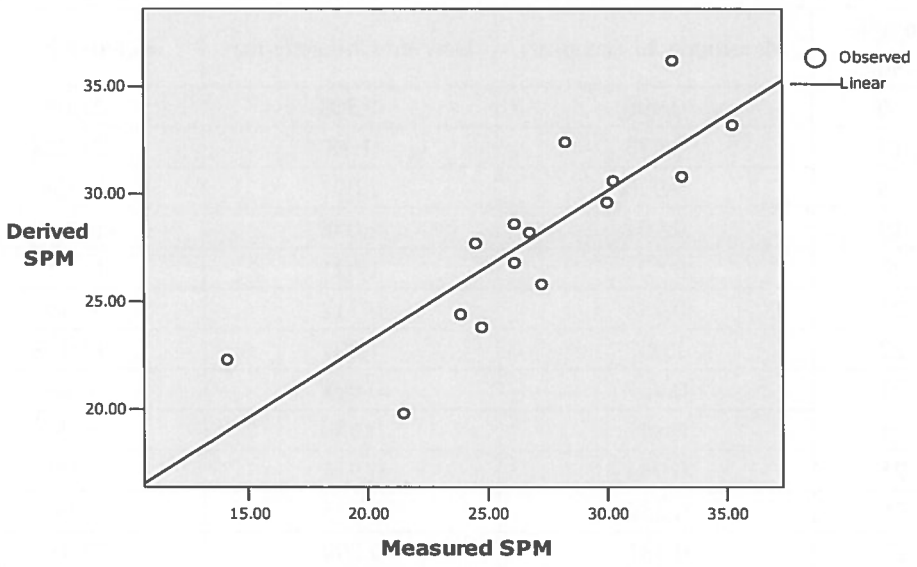

Figure 6-10 Comparison of derived and the measured SPM

Figure 6-10 is based on the linearly derived SPM concentration at 440nm. Together with table 6-20 which gives the values and relative errors of them, most of the derived SPM concentrations are close to the regression line and the relative error is less than 10.

Table 6-22 Values of Measured and Derived SPM concentration and relative errors

Sample No.	Measured SPM(mg/L)	Derived SPM(mg/L)	Relative Error
16	27.7	24.5	11.552
17	30.8	33.125	-7.548
18	28.2	26.75	5.141
19	29.6	30	-1.351
20	30.6	30.25	1.143
21	33.2	35.25	-6.174
22	36.2	32.75	9.530
23	32.4	28.25	12.808
24	28.6	26.125	8.653
25	26.8	26.125	2.518
26	24.4	23.875	2.1516
27	23.8	24.75	-3.991
28	25.8	27.25	-5.620
29	22.3	14.125	36.659
30	19.8	21.5	-8.585

6.5. Image processing

After the preprocessing and the applying of algorithm to the images, the results are shown in figures from 6-11 to 6-14. . Firstly, the backscattering coefficient of SPM is achieved. The SIOP listed in table 6-3 is used to calculate SPM from the IOP.

When the GSM model was applied into the image, the results are in the figures 6-11 and 6-12.There are very little pixels remain in the image. The lake area is not clearly found in the image since many pixels are not satisfactory linked with each other. From this map we can hardly search the SPM variation for the lake area.

Figure 6-13 is the results of neural network retrieved b_{bp}. From this map the lake area can be easily observed although the area is smaller than that in wet season. Figure 6-14 shows the variation of SPM concentration.

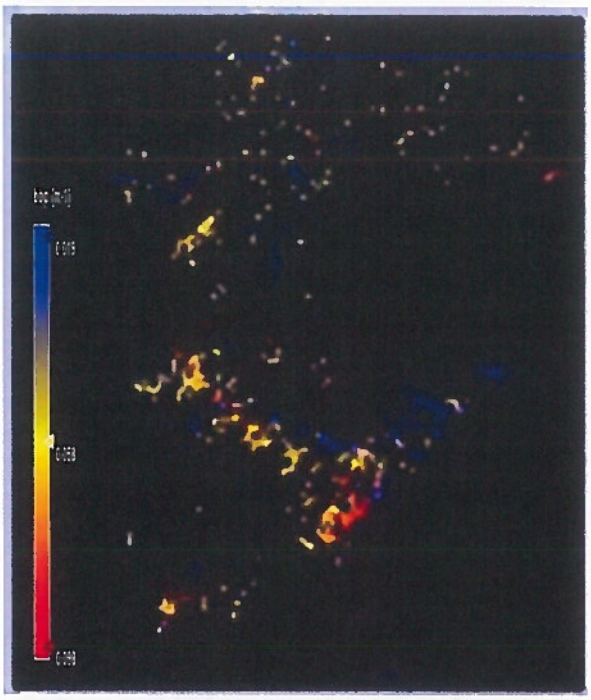

Figure 6-11 Map of backscattering coefficient of SPM

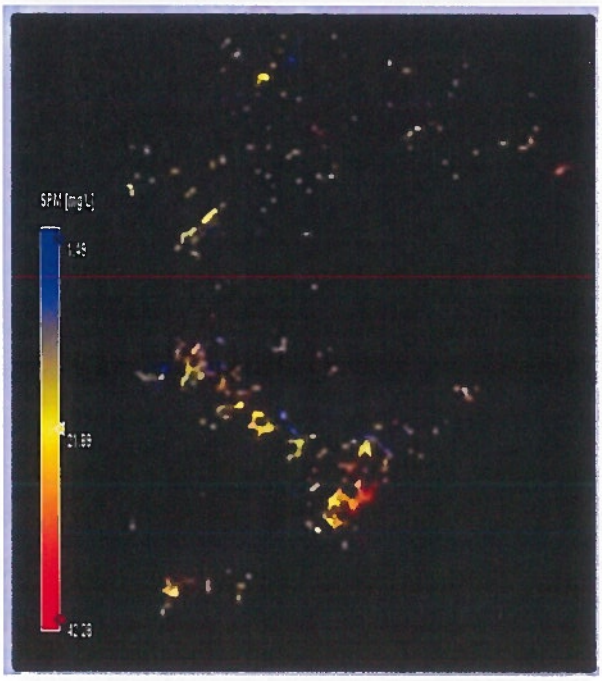

Figure 6-12 Map of SPM concentration

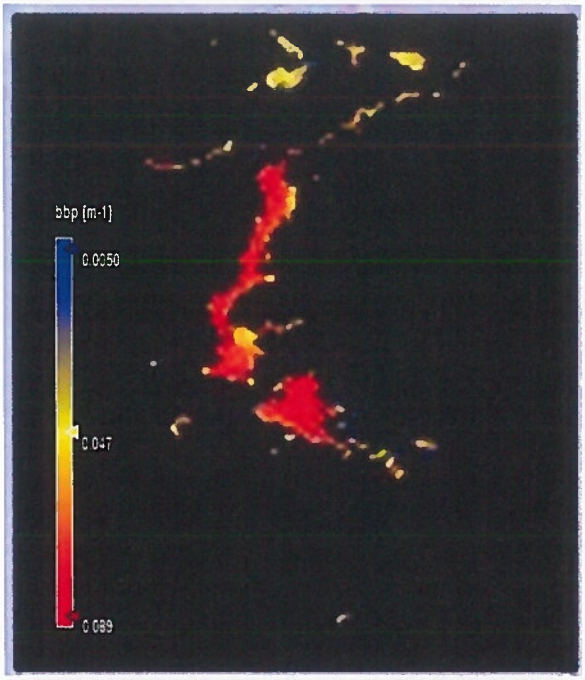

Figure 6-13 Map of backscattering coefficient of SPM

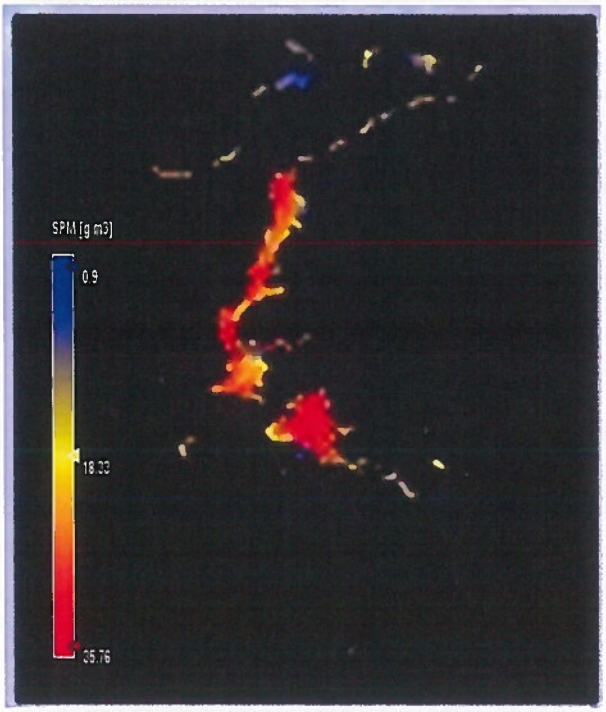

Figure 6-14 Map of SPM concentration

7. Discussion

7.1. Discussions on inverse GSM model and retrieved SIOP

(1) The measured remote sensing reflectance for the first fifteen samples is shown in figure6-1. It has a typical water spectral shape and the values are from 0.03 to 0.05. This remote sensing reflectance value is for Poyang Lake which is a turbid inland lake. For oceans, this value is always lower than for inland turbid water because they are deep and clear.

(2)After the inversion of GSM model, the backscattering coefficient of SPM b_{bp} at 440nm and the absorption coefficient of Chl-a a_{ph} at 440nm are retrieved. The value of the former is in a range of 0.04-0.1 $m^{-1}$and the latter is 0-0.2 m^{-1}.

(3) The GSM model is originally designed for ocean and some criteria should be met in order to make the model valid. The criteria are: 0<C<100mg m-3, 0<adg(443)<2.0 m-1 and 0.0001<bbp(443)<0.1 m-1. Although in our research, the target lake is turbid inland lake and the remote sensing reflectance is larger than that for the oceans, the retrieved result is still in the demanded range. Thus the model is considered valid.

(4) When calculating the SIOP for SPM, the linear, logarithmic and exponential regression methods all provide satisfactory result which indicates that there is a strong relation between the retrieved IOP and the measured concentration of water composition. Both the linear and the logarithmic ways are chosen to calculate SIOP and they will be validated in the validation section later because the samples used here is limited to retrieve a logarithmic equation and the linear way is only a little worse than so that we can hardly distinguish which one is better just from the R^2.

(5) When calculating the SIOP for Chl-a, the R^2 is not as good as for SPM which is a little less than 0.7. The RMSE varies a lot and the linear way has the lowest RMSE value (RMSE=0.209).

7.2. Discussions on inverse GSM model within bottom reflectance and retrieveSIOP

(1) The IOP retrieved in this model is to a large extent lower than that in the GSM model since in this model, it considered bottom reflectance. Some part of the above water reflectance is due to the bottom but not the water properties so the IOP is less compared with GSM model, in which the remote sensing reflectance is only a function of IOP.

(2) The outputs also contain the bottom reflectance. The original output is the bottom albedo at the wavelength of 560nm. Using the normalized shape of the bottom type in Poyang Lake the spectrum of bottom reflectance is retrieved and the value is higher than the reflectance of water.

(3) When calculate the backscattering coefficient of SPM, the R^2 is relatively lower than in GSM model and the RMSE is up to more than 3. The R^2 in linear regression is 0.590 while in exponential regression is 0.737 and we assume that the equations are reliable and can be used. Whether the SIOP can be used to derive

concentration needs to be further proved by validation.

(4) The retrieving of specific absorption coefficient of Chl-a shows bad result. In all of those three ways, the R2 is less than 0.4 and the RMSE is more than 3 which means that the relation between the derived IOP and the measured concentration is weak and can not be used in further research.

7.3. Discussions on validating the models

(1) For the retrieved SIOP for SPM in the GSM model, both linearly and logarithmic calculated SIOP are validated and the linear way turns out to be better. The R^2 reaches 0.79 and in the validating equation, the constant is close to 0 and the variables is only a little higher than 1. In the calculation of the SIOP in section 6.1, the logarithmic way has less error but here the linear way is better. The reason might be that using the limited samples, it is hard to find a nonlinear relation between the target parameters. From the result we can draw the conclusion that the GSM model and retrieved SIOP is feasible to calculated concentration of SPM.

(2) For the retrieved SIOP for Chl-a in the GSM model, the error is more than for SPM but still reliable. As the variables is around 1.2, the derived concentration is a little more than the in measured one. The relative errors listed in table6-19 showed that there is a relative big difference between the derived and the measured Chl-a concentration The error from the retrieval of Chl-a is bigger than that of SPM indicated that for the inland waters, especially in the turbid lake as Poyang Lake, the sediment is the main contribution to the reflectance thus it is more sensitive than the Chl-a and CDOM.

(3) For the validating of the model with the effect of bottom reflectance, the absorption coefficient for Chl-a is not appropriate to derive SIOP as the relation is very weak. Therefore it has not been validated here. The backscattering coefficient for SPM is used to calculate SIOP. In the validation, the R^2 is 0.69 and the RMSE is around 1.2.

(4) The impact of adding the bottom reflectance into GSM model can be seen in this section. For the deriving of SPM concentration, there is no obvious improvement of adding bottom reflectance. In validation, the GSM model without bottom reflectance shows a similar relative error as the model with bottom reflectance. But considering that in calculating SIOP, the model without bottom reflectance has higher R^2 and lower RMSE, it is more feasible in retrieving SIOP. The model with bottom reflectance is unfavorable to retrieve the absorption coefficient of Chl-a as the relation is very weak between them. For the SPM, the model shows a worse result than that in GSM model.

7.4. Discussion on image processing

(1) When applied the algorithm in GSM model to retrieve b_{bp}, there are many places that contain no data which are supposed to be lake area. The possible reason is that the atmospheric correction did not provide accuracy result. Since the GSM model relies on the water leaving radiance reflectance of each wavelength,

the inappropriate way to retrieve this remote sensing reflectance may lead to the invalid use of this model when applied to the image.

(2)When use the neural network in BEAM to retrieved bbp, the result seams reliable by showing a typical Poyang Lake area. The values of backscattering coefficient range from 0 to 0.1 and the concentration of SPM can reach to 40mg/L in some places. Most lake area contains SPM concentration of more than 18mg/L.

(3) The lake area has significantly decreased compared to the wet seasons in the previous years (Liu and Rossiter 2007). In the southern part of the lake, there is no water in the sampling period and the bottom appears out.

(4) As usual, the highest concentration of SPM occurs in the area near the southern part where the dredging activities happen mostly.

7.5. Limitations

(1) The MERIS images have fifteen bands while the first nine bands can be used to observe water composition. But in this research, only the first five bands are used. The SIOP library was built for only these bands.

(2) The adding of bottom reflectance does not improve the result. The main reason may be the limitation of bands selected into the model. From table5-5, it can be found a distinctive signal of the bottom at the NIR. This character can facilitate its retrieval.

(3) In this research, the initial bottom depth is given 10 meters at all the samples. But actually the bottom depth differs from the different samples.

(4) The bottom type is assumed to be unique and the spectrum is derived from the images which will bring errors. The way to identify bottom spectrum in this research is based on empirical comparison of spectral shape which may be inaccuracy. Also, the reflectance that derived from image may be different from what it actually is.

(5) The atmospheric correction of the model has not provided high accuracy result which lead to the invalid result of b_{bp} when applied the GSM model algorithm to the image.

8. Conclusions

The main objective of this research is to characterize the specific inherent optical properties of the Poyang Lake and quantify water turbidity using remote sensing and Semi-Analytical Bio-Optical model for shallow waters.

The field work was conducted on October 15th to 19th and 30 points were sampled. At each sample, the remote sensing reflectance was measured and the samples were brought back to Wuhan. In the laboratory of Wuhan University, the filtering of sediment is conducted and the concentrations of Chl-a and the SPM were measured by WEPI.

The GSM Semi-Analytical Bio-Optical model and the retrieved SIOP are suitable to derive the concentrations of water composition. But adding the bottom reflectance did not improve the result of deriving concentrations. The concentration maps are then achieved using MERIS images.

8.1. Conclusions on using GSM model to derive water constituents

The measured remote sensing reflectance was inverted using the GSM model to retrieve the IOP for the first half of samples from field campaign. In Matlab, the nonlinear least regression was carried out. The input into the model was the remote sensing reflectance at the first five bands in MERIS and the outputs were the absorption coefficient of CDOM at 440 nm, the backscattering coefficient of SPM at 440nm and the concentration of Chl-a. After the parameterization and calculation of these retrievals, the absorption coefficient of Chl-a and the backscattering coefficient of SPM at each bands were derived. The uncertainty of the model was also achieved in a form of the confidence intervals for the outputs.

The IOP of SPM and Chl-a was then applied to calculate the SIOP for them. For the calculating of SIOP for SPM, the R^2 showed a strong relation between the retrieved IOP and the measured concentration of it. Both the linear and the logarithmic regression methods were used and the SIOP library for each band was provided. For the SIOP of Chl-a, the relation is a little weak than that for SPM, but still reliable enough to calculate SIOP.

The validation of GSM model and the calculated SIOP was worked out by comparing the calculated concentration with the in situ concentration. If they were perfect matching each other, the model and the calculated SIOP were favorable in this case with no error. From the validating result, the calculated concentration of SPM matched the in situ very well with a high R^2 of 0.79 and the slopes closing to 1, intercepts around 0. It is also approved that the linearly calculated SIOP was better than the logarithmic way.

For the SIOP of Chl-a, the derived concentration was a little higher than the measured one.

Thus we can draw a conclusion that the GSM model, a semi-analytical ocean color model, is feasible to be used for Poyang Lake and the derived SIOP for SPM and Ch-a is reliable to calculate the concentration in this specific area.

8.2. Conclusions on adding bottom reflectance to GSM model

The effect of bottom reflectance was added into the GSM model. For shallow water, especially for Poyang Lake whose water level and area varies a lot during different seasons, the above water reflectance may be affected by the bottom reflectance. The model was inverted in the same principle as the GSM model but the output also included the bottom reflectance as well as IOP.

When calculate the SIOP using the retrieved IOP in this model and the measured concentration, big error occurred for Chl-a. The R^2 did no reach 0.4 thus the relation can not be used. For the SIOP of SPM, the relation was fine but not as good as in GSM model. Therefore, only the SIOP retrieved for SPM was considered feasible to calculate concentration. But this needs to be proved by validation.

In validation, the R^2 was 0.69 and the RMSE was more or less 1.2. From the comparison of relative errors between the derived and measured concentration of SPM in the models with and without bottom reflectance, we can hardly figure out which model is better. However, the reason that adding the bottom reflectance did not improve the result in this research may due to the limitation of selected bands into the model.

8.3. Conclusions on image processing

After the preprocessing of image, the GSM model had been inversed again while this time it was conducted on the whole image. But the result in this way showed less pixels of the lake area than it was supposed to be. The possible reason may be that a inaccuracy atmospheric correction method has been used.

Thus the neural network method in BEAM was used to retrieve the result. From the map, the range of backscattering coefficient of SPM was from 0-0.1 in the lake. The SPM concentration is up to 40mg/L. The high SPM concentration area is in the southern part of the lake.

9. Recommendations

9.1. Recommendations on using GSM model to derive water constituents

Some recommendations are listed below for the future research:

(1) Except SPM and Chl-a, the SIOP library for CDOM needs to be built. The absorption coefficient in water contains three parts. For inland lakes, it is contributed to the absorption of water, the Chl-a and the CDOM. In this research, lacking of the data on concentration of CDOM made it unreachable to calculate SIOP for CDOM. To have a complete SIOP library for Poyang Lake, the CDOM concentration is expected.
(2) To derive SIOP, use the measured IOP. In this research, the SIOP library built for SPM and Chl-a was based on the GSM model retrieved IOP and the measured concentration of water constituents. Since one of the parameters which determine the value of SIOP was from the model retrieval but not the field measurement, the result of SIOP also depended on the reliability of the model. Therefore, it is supposed that use the measured IOP and the concentration to calculate the SIOP to provide a more accuracy result.
(3)To validate the model, the measured IOP is needed as well. The direct output of the GSM model is the IOP according to the remote sensing reflectance. The model was validated together with the calculated SIOP by the measured concentration. When we validated the model, we considered the error of the retrieved SIOP as well. To have a clear result on the reliability of the model, the measured IOP is considered better as it can be compared with the output of the model.
(4) It is advisable to perform in situ measurements in many sites. Considering the limitation of time and founds, 30 samples were measured in this research. To calculate SIOP and validate the model, half of them can be used at each step. More samples are needed to find the best regression method on calculating SIOP. Additionally, it gives possibilities that more accuracy result on SIOP can be obtained.
(5) More bands can be included in SIOP library. The GSM model is first designed for SeaWiFS images but to use MERIS, more bands can be taken into consideration. If the ways to parameterize the absorption coefficient of Chl-a can be found, the first nine bands of MERIS can be involved in the model. This future sdtudy will also help us to complete the SIOP library.

9.2. Recommendations on adding bottom reflectance to GSM model

Adding the bottom reflectance in an appropriate way is critical and recommendations offered for the future study are listed below.

(1) Measure the bottom reflectance spectral shape in the field. If possible, the bottom reflectance can be measured in the field to provide accuracy spectrum of bottom reflectance. At dry season, the bottom is out of the surface and can be directly measured while at the wet season, it can be measured at the bank edge.

(2) The bottom type can be measured from place to place if it varies in the lake. It was assumed that the bottom type was unique so the input normalized bottom albedo was the same.

(3) Get the bottom depth data. As Poyang Lake is a natural wetland area, the bottom depth varies a lot not only in temporal but also in space. The average bottom depth at the sampling season was used in this study as the initial value for the model. If different bottom depths are measured at those samples, more accuracy result may come out.

(4)The sampling work can be conducted in different seasons to evaluate the effect of bottom reflectance. In dry season, the water depth is low so the bottom may have more impact on the above water reflectance. But this situation may change with the change of the bottom depth in wet season. Thus, to consider the effect of bottom reflectance in Poyang Lake, it is better that the samples cover all the seasons in a year.

9.3. Recommendations on image processing

(1) Time series images are needed. Using the result from the model, the spatial water turbidity variation has been monitored. But the temporal variation can also be showed if there are time series images. For example, these images can show whether the forbidden of dredging has improved water clarity in the future years.

(2) Measure the atmosphere parameters in the field. Many atmospheric correction models are available if some atmosphere parameters are measured in the field. In such way, a better atmospheric correction can be done which will leads to a more accuracy result on the final map.

References

Albert, A. and P. Gege (2006). "Inversion of irradiance and remote sensing reflectance in shallow water between 400 and 800 nm for calculations of water and bottom properties." Optical Optical Society of America 45: 2331-2343.

Bates, D. M. and D. G. Watts (1988). "Nonlinear regression analysis and its applications." Wiley: 365.

BEAM Development Team. (2008). "Algorithm Theoretical Basis Document MERIS Regional Case 2 water "Retrieved 7th, January, 2009, from http://www.estec.esa.nl/ftp/pub/wipsftp/WaterRadiance/Case2_water_atm_corr_ATBD.pdf.

Bricaud, A., A. Morel, et al. (1981). "Absorption by dissolved organic matter of the sea (yellow substance) in the UV and visible domains." Limnol. Oceanogr 26: 43-53.

Bukata, R. P., J. H. Jerome, et al. (1995). "Optical Properties and Remote Sening of Inland and Coastal Waters." CRC Press: Boca Raton.

Carder, K. L., S. K. Hawes, et al. (1991). "Reflectance model for quantifying chlorophyll a in the presence of productivity degradation products." J. Geophys 96: 20599-20611.

Center for Remote Sensing/GIS Application of Jiangxi Province. (2003). "The window of Poyang Lake." Retrieved 20th,July, 2008, from www.poyanglake.net.

Chen, X. L., Z. Y. Wu, et al. (2007). "Inversion Model for Dynamic Monitoring of Suspended Sediment: A Case Study on Poyang Lake." Science & Technology Review 25(6): 43-45.

Dekker, A. G., H. J. Hoogenboom, et al. (1997). "The Relation Between Inherent Optical Properties and Reflectance Spectra in Turbid Inland Waters." Remote Sensing Reviews 15: 59-74.

Duan, H. and Y. Zhang (2008). "Cyanobacteria bloom detection and monitoring from satellite observations in coastal region of Finland." Journal of Lake Sciences 20(2): 167-172.

European Space Agency. (2000-2009). "ESA Earthnet: The Medium Resolution Imaging Spectrometer Instrument." Retrieved 18th, December, 2008, from http://envisat.esa.int/instruments/meris.

European Space Agency. (2000-2009). "MERIS Products and Algorithms." Retrieved 20th, December, 2008, from http://envisat.esa.int/handbooks/meris/CNTR2.htm.

Fischer, J., R. Bennartz, et al. (1997). "ATBD Retrieval of Total Water Vapour Content." Retrieved 6th, Janurary, 2009, from http://envisat.esa.int/instruments/meris/atbd/atbd_2_04.pdf.

Fischer, J., L. Schuller, et al. (2000). "ATBD Cloud Albedo and Cloud Optical thickness." Retrieved 6th, Janurary, 2009, from http://envisat.esa.int/instruments/meris/atbd/atbd_2_01.pdf.

Fok, M. and T. Pang (2006). "Finless porpoises in Wuhan China." Newsletter of the Department of Ecology & Biodiversity 34: 18-20.

Gordon, H. R., O. B. Brown, et al. (1988). "A semianalytical radiance model of ocean color." J. Geophys 93: 10909-10924.

Gordon, H. R., O. B. Brown, et al. (1975). "Computed relationships between the inhrent and apparent optical properties of a flat homogeneous ocean." Appl.Opt. 14(2): 417-427.

IOCCG (2000). "Remote sensing of inherent optical properties: Fundamentals, Tests of Algorithms and Applications." Reports of the International Ocean-Color Coordinating Group.

IOCCG (2006). "Remote sensing of inherent optical properties: Fundamentals, Tests of Algorithms and Applications." Reports of the International Ocean-Color Coordinating Group.

Kirk, J. T. O. (1994). Light & Photosynthesis in Aquatic Ecosystem, Press Syndicate of the University of Cambridge.

Lee, Z. P., K. L. Carder, et al. (1996). "Estimating primary production at depth from remote sensing " Appl.Opt. 35: 160-166.

Lee, Z. P., K. L. Carder, et al. (1998). "Hyperspectral remote sensing for shallow waters. 1. A semianalytical model." Optical Society of America 37(27): 6329-6338.

Lee, Z. P., K. L. Carder, et al. (1999). "Hyperspectral remote sensing for shallow waters: 2. Deriving bottom depths and water properties by optimization." Optical Society of America 38(18): 3831-3843.

Li, F., W. Ji, et al. (2005). "Aerial survey of Siberian cranes in the Poyang Lake Basin." Crane Research in China: 58-65.

Li, Y. M., J. Z. Huang, et al. (2006). "Model-based remote sensing on the concentration of suspended sediments in Taihu Lake." Science of Lake 37(2).

Liu, Q. (2006). Monitoring Area Variation and Sedimentation Patterns in Poyang Lake, China Using MODIS Medium-Resolution Bands. ITC. MSc.

Liu, Q. and D. G. Rossiter (2008). "Monitoring Area Variation and Sedimentation Patterns in Poyang Lake, China Using MODIS Medium-Resolution Bands." Remote Sensing Technology and Application 23(1): 7-11.

Maritorena, S. and D. Siegel (2006). "The GSM Semi-Analytical Bio-Optical Model." IOCCG Report:No.3.Canada:International Ocean-Colour Coordinating Group.

Maritorena, S., D. Siegel, et al. (2002). "Optimization of a semi-analytical ocean color model for global-scale application." Appl.Opt. 41: 2705-2714.

Maritorena, S. and D. A. Siegel (2005). "Consistent merging of satellite ocean color data sets using a bio-optical model." Remote Sensing of Environment 94: 429-440.

Miller, R. L. and B. A. McKee (2004). "Using MODIS Terra 250 m imagery to map concnetrations of total suspended matter in coastal waters." Remote Sensing of Environment 93: 259-266.

Morel, A. and H. R. Gordon (1983). "Remote sensing assessment of ocean color for interpretation of satellite visible imagery: a review." Springer-Verlag: 44.

Mueller, J. L., G. S. Fargion, et al. (2003). Ocean Optics Protocols For Satellite Ocean Color Sensor Validation, Revision 4, NASA.

National Environmental Protection Bureau (2006). Methods on monitoring water and sewage, Xinhua.

Nelson, N. B. and D. A. Siegel (2002). "Chromophoric DOM in the open ocean." Biogeochemistry of Marine Dissolved Organic Matter: 774.

Nelson, N. B., D. A. Siegel, et al. (1998). "Seasonal dynamics of colored dissolved material in the Sargasso Sea." Deep-Sea 45: 931-957.

Pietro, A. B., G. Claudia, et al. (2001). "Validation of satellite data for quality assurance in lake monitoring applications." The Science of the Total Environment 268: 3-18.

Pope, R. and E. Fry (1997). "Absorption spectrum (380-700nm) of pure waters:Integrating cavity measurements." Appl.Opt. 36: 8710-8723.

Ritchie, J. C. and C. M. Cooper (1998). "Comparison of measured suspended sediment concentration with suspended concentration estimated from Landsat MSS data." Remote Sensing 9(3): 379-387.

Ritchie, J. C. and F. R. Schiebe (1998). "Water quality: remote sensing in hydrology and water management " Edwin T Engan.

Ritchie, J. C., F. R. Schiebe, et al. (1996). "Remote sensing of suspended sediment in surface water." Photographic Engineering Remote Sensing 42: 1539-1545.

Senar, J. C. and A. Borras (2004). "Surviving to winter: Strategies of wintering birds in the Iberian Peninsula." Ardeola 51(1): 133-168.

Smith, R. C. and K. S. Baker (1981). "Optical properties of the clearest natural waters." Appl.Opt. 20: 177-184.

Tang, J. W., G. L. Tian, et al. (2004). "The spectral measurement and analysis of water 1: above water mesurement (in Chinese)." Journal of Remote Sensing 8(1).

Wu, G., J. de Leeuw, et al. (2007). "Concurrent monitoring of vessels and water turbidity enhances the strength of evidence in remotely sensed dredging impact assessment." Water Research 41(15): 3271-3280.

Zhong, Y. and S. Chen (2005). "Imapct of the dredging on fish in Poyang Lake." Jiangxi Fishery Sciences and Technology(1): 15-18.

Appendix A Field Survey

No.	Time		water temperature(°C)	latitude	longitude
1	15th Oct	10:05am	24.3	29°15.394′	116°04.430′
2		10:35am	24.5	29°14.794′	116°05.314′
3		10:51am	23.5	29°14.253′	116°06.073′
4		11:19am	24.6	29°13.705′	116°07.519′
5		11:41am	25	29°13.158′	116°09.161′
6		12:08am	24.8	29°12.586′	116°11.373′
7		12:21am	24.7	29°12.049′	116°11.460′
8		12:34am	24.8	29°11.501′	116°11.501′
9		12:47am	24.9	29°11.065′	116°11.870′
10		1:01pm	26.2	29°10.544′	116°12.009′
11		1:21pm	26.2	29°11.338′	116°12.610′
12		1:36pm	25.8	29°11.981′	116°12.897′
13		1:54pm	25.5	29°12.564′	116°12.725′
14		2:27pm	25.4	29°13.270′	116°11.453′
15		2:39pm	24.7	29°13.301′	116°12.046′
16	18th Oct	1:00pm	26.2	29°23.556′	116°01.762′
17		1:16pm	25.2	29°23.017′	116°02.486′
18		1:30pm	24.8	29°22.468′	116°03.173′
19		1:46pm	24.2	29°21.963′	116°03.577′
20		2:14pm	24.8	29°21.370′	116°03.821′
21		2:34pm	24.6	29°20.770′	116°03.830′
22		3:00pm	24.5	29°20.246′	116°03.747′
23	19th Oct	10:20am	24	29°20.026′	116°03.557′
24		10:57am	24.1	29°19.207′	116°03.303′
25		11:31am	24.4	29°18.624′	116°03.090′
26		11:48am	24.8	29°18.070′	116°02.915′
27		12:06am	24.8	29°17.519′	116°02.884′
28		12:20am	25.1	29°16.978′	116°03.243′
29		12:36am	25.2	29°16.440′	116°03.481′
30		12:59am	25.8	29°15.908′	116°03.726′

Appendix B Laboratory analysis of SPM concentration

NO.	Volume(ml)	Concentration(mg/l)
1	250	22.5
2	250	23.8
3	350	19.7
4	150	13.4
5	300	35.7
6	400	18.4
7	250	23.8
8	250	29.2
9	350	25
10	400	21.2
11	250	29.1
12	300	29.8
13	250	26.8
14	250	23.2
15	150	25.9
16	200	27.7
17	250	30.8
18	250	28.2
19	250	29.6
20	250	30.6
21	250	33.2
22	200	36.2
23	150	32.4
24	150	28.6
25	250	26.8
26	250	24.4
27	250	23.8
28	200	25.8
29	250	22.3
30	250	19.8

Appendix C Laboratory analysis of Chl-a concentration

NO.	Volume(ml)	Concentration(mg/m3)
1	500	0.639
2	500	0.703
3	400	0.662
4	450	0.207
5	500	1.521
6	500	0.908
7	500	1.028
8	500	1.469
9	500	1.218
10	500	1.098
11	500	1.14
12	500	1.206
13	500	1.113
14	500	0.863
15	500	0.669
16	500	0.998
17	500	0.973
18	400	0.996
19	500	0.907
20	500	0.922
21	500	0.735
22	500	1.052
23	450	0.927
24	300	0.847
25	500	0.944
26	500	0.854
27	500	0.731
28	500	1.057
29	500	0.62
30	500	0.768